Effect of the $N\Delta$ interaction on observables of the πNN and γNN systems

M. T. Peña
Centro de Física Nuclear da Universidade de Lisboa (INIC), 1699 Lisboa Codex, Portugal

H. Garcilazo
Theoretical Physics, University of Hannover, D-3000 Hannover, Germany

U. Oelfke
TRIUMF, 4004 Wesbrook Mall, Vancouver, British Columbia, Canada V6T2A3

P. U. Sauer
Theoretical Physics, University of Hannover, D-3000 Hannover, Germany
and Nuclear Theory Group, Department of Physics, FM-15, University of Washington, Seattle, Washington 98195
(Received 1 July 1991)

Effects on the hadronic and electromagnetic properties of the two-nucleon system above pion threshold, arising from the interaction of the Δ isobar with nucleons, are investigated. The instantaneous nucleon-Δ potential is based on the meson exchange. Two-body reactions connecting channels with at most one pion and one photon are studied. Processes leading to a three-body pion-two-nucleon final state are considered in the restricted kinematic domain in which the pion forms the P_{33} resonance with one of the nucleons. The nucleon-Δ potential is seen to increase the relative importance of the inelastic strength of two-nucleon spin-triplet states with respect to spin-singlet states, correcting a deficiency common in most existing models. Theoretical predictions are compared with recent experimental data for the various reactions. In particular, the differential cross section and the proton beam asymmetry for $pp \rightarrow n\Delta^{++}$ ($p\pi^+$) are calculated, the latter observable being especially sensitive to the nucleon-Δ interaction.

PACS number(s): 13.75.Cs, 21.30.+y, 21.45.+v

I. INTRODUCTION

The Δ isobar is the most important mode of nucleonic excitation at intermediate energies. In the nuclear medium, it yields structure corrections for the traditional description of nuclear properties in terms of nucleonic degrees of freedom only, and it is an important reaction mechanism for hadronic and electromagnetic (e.m.) processes. Thus the interaction between the Δ isobar and nucleon (N) should be most important for any theoretical description of nuclear phenomena at intermediate energies. However, the interaction is theoretically poorly known, its theoretical significance is hardly proved, and theoretic models for the interaction are therefore experimentally not tested.

This paper adopts a meson-exchange model for the instantaneous nucleon-Δ potential. The exchanged mesons taken into account are the pion (π), the sigma (σ), the rho (ρ), and the omega (ω). The contribution of that nucleon-Δ potential to the three-nucleon force in the three-nucleon bound state is studied in Ref. [1]. In the present paper, its effect on the two-nucleon system above pion threshold is discussed.

Hadronic and e.m. processes connecting two-nucleon channels with at most one pion and one photon (γ) are investigated, i.e., reactions starting from the NN, pion-deuteron (πd), and photon-deuteron (γd) channels and leading to the NN, πd, and πNN channels, which are all unitarily coupled. The processes yielding a three-body final state are considered only in the kinematic domain [2] in which the pion forms the P_{33} resonance with one of the nucleons. Two force models are compared in their effect on the observables of those reactions: In one, the instantaneous nucleon-Δ potential is included; in the other, it is switched off.

Section II gives the theoretical framework according to which the calculation proceeds, Sec. II A recalls the scattering theory for the hadronic reactions, and Sec. II B for the e.m. reactions, whereas Sec. II C describes the actual parametrization of the interaction models. The results are presented in Sec. III and conclusions in Sec. IV.

II. THEORETICAL FRAMEWORK

The considered reactions are theoretically described as in Ref. [3] in an extended Hilbert space $\mathcal{H}=\mathcal{H}_N\oplus\mathcal{H}_\Delta\oplus\mathcal{H}_\pi$ with nonnucleonic degrees of freedom. The nucleonic sector is $\mathcal{H}_N$, in $\mathcal{H}_\Delta$ one of the nucleons is replaced by a Δ isobar, and in $\mathcal{H}_\pi$ a single pion is added to purely nucleonic configurations. The projectors on the three different sectors $\mathcal{H}_N$, $\mathcal{H}_\Delta$, and $\mathcal{H}_\pi$ of the Hilbert space are P_N, P_Δ, and Q, respectively.

According to Ref. [3], the Δ isobar of the sector $\mathcal{H}_\Delta$ is an undressed baryon with spin $\frac{3}{2}$, isospin $\frac{3}{2}$, and mass $m_\Delta=1315$ MeV. Only by its coupling to pion-nucleon states does it become the physical P_{33} resonance; that

coupling yields self-energy corrections

$$\Sigma_\Delta(\varepsilon_\Delta,k_\Delta)=M(\varepsilon_\Delta,k_\Delta)c^2+\frac{k_\Delta^2}{2m_\Delta}-\frac{i}{2}\Gamma_\Delta(\varepsilon_\Delta,k_\Delta)\ , \quad (2.1)$$

for the Δ isobar, i.e., a corrected mass $M_\Delta(\varepsilon_\Delta,k_\Delta)$ and a width $\Gamma_\Delta(\varepsilon_\Delta,k_\Delta)$, which depend on its momentum k_Δ and on the energy ε_Δ available for its decay into pion-nucleon states.

The dynamics is controlled by the Hamiltonian

$$H=H_0+H_1\ , \quad (2.2a)$$

whose kinetic-energy part H_0 defines the basis states in the three sectors of Hilbert space and whose interaction part H_1 is chosen to be

$$H_1=(P_N+P_\Delta)H_1(P_N+P_\Delta) +P_\Delta H_1 Q+QH_1P_\Delta+QH_1Q\ , \quad (2.2b)$$

the lattice choice takes $P_NH_1Q=QH_1P_N=0$. Therefore nucleons are not allowed to emit or absorb pions directly; pions are considered to be emitted or absorbed only in a two-step mechanism mediated by Δ deexcitation or Δ excitation. The reaction mechanism is the same as the one employed in Ref. [4]. The different building blocks of the interaction H_1 are illustrated in Fig. 1. The part $P_\Delta H_1 P_\Delta$ is the instantaneous nucleon-Δ potential, whose effect is studied in the present paper.

The e.m. interaction is parametrized as in Refs. [5] and [6]. The e.m. Hamiltonian

$$H_1^\gamma=\int d^3x A^\mu(\mathbf{x})j_\mu(\mathbf{x}) \quad (2.3)$$

connects the hadronic current $j^\mu(\mathbf{x})$ to the external photon field $A^\mu(\mathbf{x})$. The current is assumed to have one- and two-baryon pieces, i.e., $j^\mu(\mathbf{x})=j^{[1]\mu}(\mathbf{x})+j^{[2]\mu}(\mathbf{x})$. It acts in the different sectors of the Hilbert space and couples them, i.e.,

$$j^\mu(\mathbf{x})=(P_N+P_\Delta+Q)j^\mu(\mathbf{x})(P_N+P_\Delta+Q)\ . \quad (2.4)$$

There are nine distinct channel couplings, each possibly of one- and two-baryon nature and two-baryon parts with distinct dynamic structures. Figure 2 shows only those parts $P_Nj^\mu(\mathbf{x})P_N$, $P_\Delta j^\mu(\mathbf{x})P_N$, from which the current for the present calculation will be chosen.

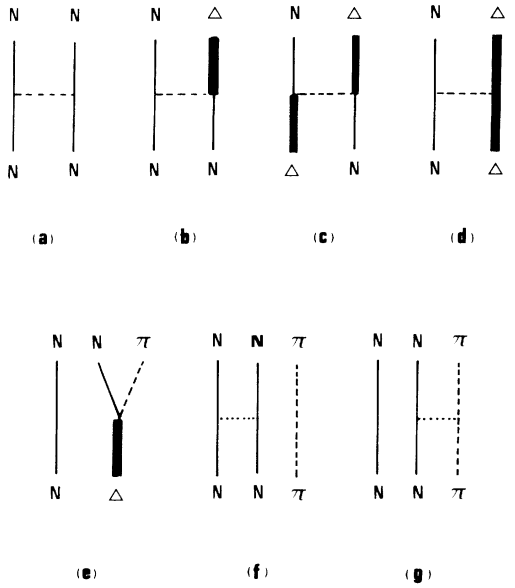

FIG. 1. Driving terms of the hadronic part of the extended Hilbert-space Hamiltonian $\mathcal{H}$. Processes (a)–(d) show the two-body potentials in the pure baryonic sector $\mathcal{H}_N\oplus\mathcal{H}_\Delta$. Process (e) relates the Δ-isobar sectors through the $\pi N\Delta$ vertex and processes (f) and (g) are the interactions in the pionic sector of the Hilbert space.

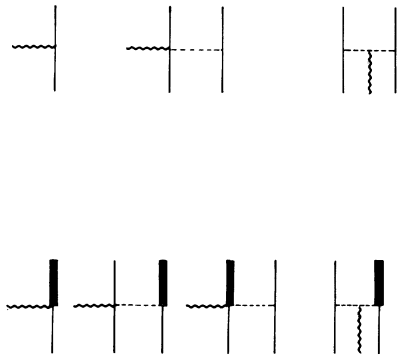

FIG. 2 Part of the e.m. current. Only two particular channel couplings are shown, i.e., the diagonal nucleonic current $P_Nj^\mu(x)P_N$ and the transition current $P_\Delta j^\mu(x)P_N$ from purely nucleonic states to states with one Δ isobar. One- and two-baryon contributions, i.e., $j^{[1]\mu}(x)$ and $j^{[2]\mu}(x)$, arise. The two-baryon contribution $P_\Delta j^{[2]\mu}(x)P_N$ to the transition current will not be included in the calculation of this paper.

A. Description of the hadronic reactions

The description of the hadronic reactions uses the Alt-Grassberger-Sandhas (AGS) three-particle scattering theory [7] extended to accommodate particle absorption as in Ref. [3]. The description of Ref. [3] is almost identical to the approach of Ref. [4] and very similar to the approaches of Refs. [8–14]. The whole literature is summarized in Ref. [15]. In the present paper, we study the effect of the instantaneous nucleon-Δ potential $P_\Delta H_1 P_\Delta$ on the observables of the considered processes. Compared with Ref. [3], we simplify the force model by choosing all interactions in the Hilbert sector with a pion to be zero, i.e., $QH_1Q=0$. This choice is a serious approximation on the physics content of the force model. Furthermore, it is *inconsistent* with an asymptotic pion-deuteron channel and therefore, for deuteron reactions, also a violation of unitarity. We take the general results of scattering theory from Ref. [3] and will specialize them to the approximation $QH_1Q=0$.

The S matrix connects the two-nucleon, the pion-deuteron, and the πNN three-body breakup channels. The corresponding initial and final plane-wave channel states, i.e., $|\phi_i\rangle$ and $|\phi_f\rangle$, are, respectively, $|\phi_N(\mathbf{p}_N)\rangle$, of energy $E_N=2e_N(p_N)$, with two-nucleon relative momentum $\mathbf{p}_N$ and single-nucleon energies

$e_N(p_N)=m_Nc^2+p_N^2/2m_N$, $|\phi_\pi(\mathbf{q}_\pi)\rangle$, of energy $E_\pi=e_d(q_\pi)+\omega_\pi(q_\pi)$, with pion-deuteron relative momentum $\mathbf{q}_\pi$ and deuteron and pion energies $e_d(q_\pi)$ and $\omega_\pi(q_\pi)$ given by $e_d(q_\pi)=2m_Nc^2+\varepsilon_d+q_\pi^2/4m_N$ (ε_d stands for the deuteron binding energy) and $\omega_\pi(q_\pi)=(m_\pi^2c^4+q_\pi^2c^2)^{1/2}$, and $|\phi_0(p,q)\rangle$ of energy E_0 with relative three-particle momenta $\mathbf{p}$ and $\mathbf{q}$ to be defined as in Ref. [3]. The required S-matrix elements $\langle\phi_f|S|\phi_i\rangle$ are given in terms of the multichannel transition matrix $U(z)$, whose on-energy-shell elements yield the physical scattering amplitudes and, therefore, cross sections directly. The transition matrix $U(z)$ depends on the Hamiltonian H and is determined by integral equations. As in Ref. [3], we choose the one for its two-baryon components, i.e.,

$$U_{ba}(z)=\sum_{c=N,\Delta}P_b\left[H_1+H_1Q\frac{Q}{z-QH_0Q}QH_1\right]P_c\times\left[\delta_{ca}+\frac{P_c}{z-P_cH_0P_c}U_{ca}(z)\right], \quad (2.5)$$

as the basic equation, from which all other elements will be derived. The Latin lower-case letters a, b, and c denote the two-nucleon channel N and the nucleon-Δ channel Δ. The part of the driving term arising from the pionic channel, i.e.,

$$P_bH_1Q\frac{Q}{z-QH_0Q}QH_1P_a=[P_b\delta H_0(z)P_a+P_b\delta H_1(z)P_a]\delta_{ba}\delta_{\Delta a}, \quad (2.6)$$

has disconnected one-baryon and connected two-baryon contributions $P_b\delta H_0(z)P_a$ and $P_b\delta H_1(z)P_a$, respectively, which are channel diagonal and nonvanishing in the nucleon-Δ channel Δ only, because of the approximation $P_NH_1Q=QH_1P_N=0$. As seen in Ref. [3], the two-baryon components $U_{ba}(z)$ are therefore numerically simpler determined from the two-baryon auxiliary transition matrix $T_{ba}(z)$ in the form

$$U_{ba}(z)=\left[P_b\delta H_0(z)P_b+P_b\delta H_0(z)P_b\frac{P_b}{z-P_b[H_0+\delta H_0(z)]P_b}\right]\delta_{ba}\delta_{\Delta a}+\left[P_b+P_b\delta H_0(z)P_b\frac{P_b}{z-P_b[H_0+\delta H_0(z)]P_b}\right]T_{ba}(z)\left[P_a+\frac{P_a}{z-P_a[H_0+\delta H_0(z)]P_a}P_a\delta H_0(z)P_a\right]. \quad (2.7)$$

The obvious advantage of Eq. (2.7) is that all one-baryon contributions are collected in the first term, whereas the auxiliary transition matrix $T_{ba}(z)$ follows from an integral equation with a connected two-baryon driving term $P_b[H_1+\delta H_1(z)]P_a$ and a propagator incorporating the self-energy corrections for the Δ isobar in the nucleon-Δ channel according to

$$T_{ba}(z)=\sum_{c=N,\Delta}P_b[H_1+\delta H_1(z)]P_c\left[\delta_{ca}+\frac{P_c}{z-P_c[H_0+\delta H_0(z)]P_c}T_{ca}(z)\right]. \quad (2.8)$$

The elastic two-nucleon scattering amplitude is identical with the auxiliary transition matrix, i.e.,

$$U_{NN}(z)=T_{NN}(z). \quad (2.9)$$

All other components of the multichannel transition matrix $U(z)$, required for the description (2.5) of the hadronic reactions, can be related to the transition-matrix components $U_{ba}(z)$ of the two-baryon channels and therefore to the auxiliary two-baryon transition matrix $T_{ba}(z)$ in turn, i.e.,

$$U_{\pi N}(z)=QH_1P_\Delta\frac{P_\Delta}{z-P_\Delta[H_0+\delta H_0(z)]P_\Delta}T_{\Delta N}(z), \quad (2.10)$$

$$U_{0N}(z)=QH_1P_\Delta\frac{P_\Delta}{z-P_\Delta[H_0+\delta H_0(z)]P_\Delta}T_{\Delta N}(z), \quad (2.11)$$

$$U_{N\pi}(z)=T_{N\Delta}(z)\frac{P_\Delta}{z-P_\Delta[H_0+\delta H_0(z)]P_\Delta}P_\Delta H_1Q, \quad (2.12)$$

$$U_{\pi\pi}(z)=QH_1P_\Delta\left[\frac{P_\Delta}{z-P_\Delta[H_0+\delta H_0(z)]P_\Delta}+\frac{P_\Delta}{z-P_\Delta[H_0+\delta H_0(z)]P_\Delta}T_{\Delta\Delta}(z)\frac{P_\Delta}{z-P_\Delta[H_0+\delta H_0(z)]P_\Delta}\right]P_\Delta H_1Q, \quad (2.13)$$

$$U_{0\pi}(z)=QH_1P_\Delta\left[\frac{P_\Delta}{z-P_\Delta[H_0+\delta H_0(z)]P_\Delta}+\frac{P_\Delta}{z-P_\Delta[H_0+\delta H_0(z)]P_\Delta}T_{\Delta\Delta}(z)\frac{P_\Delta}{z-P_\Delta[H_0+\delta H_0(z)]P_\Delta}\right]P_\Delta H_1Q\ . \tag{2.14}$$

The results (2.9)–(2.14) are taken from Ref. [3]. The approximation $QH_1Q=0$ is implemented into the integral equations (2.5) and (2.8) for $U_{ba}(z)$ and $T_{ba}(z)$ and into the relations (2.9)–(2.14) between the multichannel components of the transition matrix $U(z)$. One notes that the approximation $QH_1Q=0$ yields the operator identities $U_{\pi N}(z)=U_{0N}(z)$ and $U_{\pi\pi}(z)=U_{0\pi}(z)$. Only the asymptotic channel states will distinguish their matrix elements.

The derivation of cross sections from the transition matrix $U(z)$ is standard for most reactions. In the two processes $NN\to\pi NN$ and $\pi d\to\pi NN$, leading to three-body final states, the differential cross sections are

$$d^6\sigma_{pp\to(\pi^+p)n}=(2\pi)^4\frac{\mu_N(p_N)}{\hbar^2}\frac{1}{p_N}\delta(E_0'-E_N)|\langle\phi_0(\mathbf{p}',\mathbf{q}')|U_{0N}(E_N+i0)|\phi_N(\mathbf{p}_N)\rangle|^2d^3p'\,d^3q'\ , \tag{2.15a}$$

$$d^6\sigma_{\pi^+d\to(\pi^+p)n}=(2\pi)^4\frac{\mu_\pi(q_\pi)}{\hbar^2}\frac{1}{q_\pi}\delta(E_0'-E_\pi)|\langle\phi_0(\mathbf{p}',\mathbf{q}')|U_{0\pi}(E_\pi+i0)|\phi_\pi(\mathbf{q}_\pi)\rangle|^2d^3p'\,d^3q'\ , \tag{2.15b}$$

where

$$\mu_N(p_N)c^2=\tfrac{1}{2}(m_N^2c^4+p_N^2c^2)^{1/2}$$

and

$$\mu_\pi(q_\pi)c^2=\frac{\omega_d(q_\pi)\omega_\pi(q_\pi)}{\omega_d(q_\pi)+\omega_\pi(q_\pi)}\ ,$$

with $\omega_d(q_\pi)c^2=(m_d^2c^4+q_\pi^2c^2)^{1/2}$, are the reduced masses in the initial two-nucleon and pion-deuteron channels. The dependence of the cross sections on spin and isospin is not made explicit in Eq. (2.15). Both processes will be discussed for the restricted kinematic domain in which the pion forms the P_{33} resonance with one of the nucleons, the spins of the participating particles not being observed. The differential cross sections take the form

$$\frac{d\sigma_{pp\to(\pi^+p)n}}{d\Omega_{q'}}=2(2\pi)^4\frac{\mu_N(p_N)}{\hbar^2}\frac{1}{p_N}\sum_{\text{spin}}\left[-\frac{1}{\pi}\right]\int q'^2dq'\left[\text{Im}\frac{1}{E_N+i0-e_N(q')-\Sigma_\Delta(E_N-e_N(q'),q')}\right]$$
$$\times|\langle\mathbf{q}'|T_{\Delta N}(E_N+i0)|\mathbf{p}_N\rangle|^2\ , \tag{2.16a}$$

$$\frac{d\sigma_{\pi^+d\to(\pi^+p)n}}{d\Omega_{q'}}=2(2\pi)^4\frac{\mu_\pi(q_\pi)}{\hbar^2}\frac{1}{q_\pi}\sum_{\text{spin}}\left[-\frac{1}{\pi}\right]\int q'^2dq'\left[\text{Im}\frac{1}{E_\pi+i0-e_N(q')-\Sigma_\Delta(E_\pi-e_N(q'),q')}\right]$$
$$\times|\langle\mathbf{q}'|T_{\Delta\pi}(E_\pi(q_\pi)+i0)|\mathbf{q}_\pi\rangle|^2\ , \tag{2.16b}$$

where $\Omega_{q'}$ is the direction of the resonating (π^+p) system. In Eq. (2.16b) the shorthand notation

$$T_{\Delta\pi}(z)=\left[1+T_{\Delta\Delta}(z)\frac{P_\Delta}{z-P_\Delta[H_0+\delta H_0(z)]P_\Delta}\right]P_\Delta H_1Q \tag{2.16c}$$

is introduced which will—as discussed in Appendix A—also provide a computational advantage. Since

$$-\text{Im}[z-\Sigma_\Delta(z,k_\Delta)]^{-1}=\tfrac{1}{2}\Gamma_\Delta(z,k_\Delta)\{[z-k_\Delta^2/2m_\Delta-M_\Delta(z,k_\Delta)]^2+\tfrac{1}{4}\Gamma_\Delta^2(z,k_\Delta)\}^{-1}\ ,$$

the differential cross sections (2.16), as well as the spin-dependent observables such as the beam asymmetry A_y, show the same averaging over the width of the P_{33} resonance as introduced in Ref. [16] for extracting nucleon-Δ phase shifts. The derivation of Eq. (2.16) is given in Appendix B.

B. Description of e.m. reactions

For the description of the e.m. reactions, the main results are taken from Refs. [5] and [6]. In one-photon exchange the S-matrix elements $\langle\phi_f|S|d(-\mathbf{k}_\gamma)\gamma\mathbf{k}_\gamma\rangle$ for photon absorption on the deuteron are determined by the corresponding matrix elements of the e.m. interaction $\langle\psi_f^{(-)}|H_1^\gamma|d(-\mathbf{k}_\gamma)\rangle$. The indicated matrix elements refer to the c.m. system of the whole process: $|d(-\mathbf{k}_\gamma)\rangle$ represents the deuteron state moving with momentum $-\mathbf{k}_\gamma$, where $\mathbf{k}_\gamma$ is the momentum of the photon state $|\gamma\mathbf{k}_\gamma\rangle$, $|\phi_f\rangle$, with $f=N,\pi,0$ the asymptotic hadronic channel states introduced in Sec. II A, whereas $|\psi_f^{(\pm)}\rangle$ with $f=N,\pi,0$ denote the fully correlated scattering states. The latter states are determined by the

half-shell elements of the multichannel transition matrix $U(z)$ and evolve from the respective asymptotic channel states $|\phi_f\rangle$ according to

$$|\psi_N^{(\pm)}(\mathbf{p}_N)\rangle = \frac{\pm i0}{E_N \pm i0 - H}|\phi_N(\mathbf{p}_N)\rangle \ , \tag{2.17a}$$

$$|\psi_N^{(\pm)}(\mathbf{p}_N)\rangle = \left[P_N + \frac{P_N}{E_N \pm i0 - P_N H_0 P_N} U_{NN}(E_N \pm i0) + \left[P_\Delta + \frac{Q}{E_N \pm i0 - QH_0Q} QH_1P_\Delta\right] \frac{P_\Delta}{E_N \pm i0 - P_\Delta H_0 P_\Delta} U_{\Delta N}(E_N \pm i0)\right] |\phi_N(\mathbf{p}_N)\rangle \ , \tag{2.17b}$$

$$|\psi_\pi^{(\pm)}(\mathbf{q}_\pi)\rangle = \frac{\pm i0}{E_\pi \pm i0 - H}|\phi_\pi(\mathbf{q}_\pi)\rangle \ , \tag{2.18a}$$

$$|\psi_\pi^{(\pm)}(\mathbf{q}_\pi)\rangle = \left[\frac{P_N}{E_\pi \pm i0 - P_N H_0 P_N} U_{N\pi}(E_\pi \pm i0) + \frac{P_\Delta}{E_N \pm i0 - P_\Delta H_0 P_\Delta} U_{\Delta\pi}(E_\pi \pm i0) + \left[Q + \frac{Q}{E_\pi \pm i0 - QH_0Q} U_{\pi\pi}(E_\pi \pm i0)\right]\right] |\phi_\pi(\mathbf{q}_\pi)\rangle \ , \tag{2.18b}$$

$$|\psi_0^{(\pm)}(\mathbf{p},\mathbf{q})\rangle = \frac{\pm i0}{E_0 \pm i0 - H}|\phi_0(\mathbf{p},\mathbf{q})\rangle \ , \tag{2.19a}$$

$$|\psi_0^{(\pm)}(\mathbf{p},\mathbf{q})\rangle = \left[\frac{P_N}{E_0 \pm i0 - P_N H_0 P_N} U_{N0}(E_0 \pm i0) + \frac{P_\Delta}{E_0 \pm i0 - P_\Delta H_0 P_\Delta} U_{\Delta 0}(E_0 \pm i0) + \left[Q + \frac{Q}{E_0 \pm i0 - QH_0Q} U_{00}(E_0 \pm i0)\right]\right] |\phi_0(\mathbf{p},\mathbf{q})\rangle \ . \tag{2.19b}$$

Replacing the multichannel transition matrix $U(z)$ in terms of the connected auxiliary two-baryon transition matrix $T_{ba}(z)$, according to Eq. (2.7), the matrix elements of the e.m. interaction take the following specific forms for the photon-deuteron reactions leading to two-nucleon, pion-deuteron, and pion–two-nucleon breakup final states, i.e.,

$$\langle \psi_N^{(-)}(\mathbf{p}'_N)|H_1^\gamma|d(-\mathbf{k}_\gamma)\rangle = \langle \phi_N(\mathbf{p}'_N)| \left[P_N + T_{NN}(E'_N + i0)\frac{P_N}{E'_N + i0 - P_N H_0 P_N} + T_{N\Delta}(E_N + i0)\frac{P_\Delta}{E'_N + i0 - P_\Delta[H_0 + \delta H_0(E'_N + i0)]P_\Delta} \times \left[P_\Delta + P_\Delta H_1 Q \frac{Q}{E'_N + i0 - QH_0Q}\right]\right] H_1^\gamma P_N |d(-\mathbf{k}_\gamma)\rangle \ , \tag{2.20}$$

$$\langle \psi_\pi^{(-)}(\mathbf{q}'_\pi)|H_1^\gamma|d(-\mathbf{k}_\gamma)\rangle = \langle \phi_\pi(\mathbf{q}'_\pi)| \left\{Q + QH_1P_\Delta \frac{P_\Delta}{E'_\pi + i0 - P_\Delta[H_0 + \delta H_0(E'_\pi + i0)]P_\Delta} \times \left[T_{\Delta N}(E'_\pi + i0)\frac{P_N}{E'_\pi + i0 - P_N H_0 P_N} + \left[P_\Delta + T_{\Delta\Delta}(E'_\pi + i0)\frac{P_\Delta}{E'_\pi + i0 - P_\Delta[H_0 + \delta H_0(E'_\pi + i0)]P_\Delta}\right] \times \left[P_\Delta + P_\Delta H_1 Q \frac{Q}{E'_\pi + i0 - QH_0Q}\right]\right]\right\} H_1^\gamma P_N |d(-\mathbf{k}_\gamma)\rangle \ , \tag{2.21}$$

$$\langle \psi_0^{(-)}(\mathbf{p}',\mathbf{q}')|H_1^\gamma|d(-\mathbf{k}_\gamma)\rangle = \langle \phi_0(\mathbf{p}',\mathbf{q}')| \left\{ Q + QH_1P_\Delta \frac{P_\Delta}{E_0'+i0-P_\Delta[H_0+\delta H_0(E_0'+i0)]P_\Delta} \times \left[T_{\Delta N}(E_0'+i0)\frac{P_N}{E_0'+i0-P_N H_0 P_N} + \left[P_\Delta + T_{\Delta\Delta}(E_0'+i0)\frac{P_\Delta}{E_0'+i0-P_\Delta[H_0+\delta H_0(E_0'+i0)]P_\Delta} \right] \times \left[P_\Delta + P_\Delta H_1 Q \frac{Q}{(E_0'+i0-QH_0Q)} \right] \right] \right\} H_1^\gamma P_N |d(-\mathbf{k}_\gamma)\rangle \ . \quad (2.22)$$

The relative momenta and energies of all particles in final states are marked with a prime. The effective operators in Eqs. (2.21) and (2.22) leading to the two-body pion-deuteron and three-body breakup final states are identical because of the approximation $QH_1Q=0$. Only the final channel states distinguish their matrix elements. This result corresponds to the operator identity already encountered for those components of the multichannel hadronic transition matrix $U(z)$, yielding to the two-body pion-deuteron and three-body breakup final states. For the actual calculation of the matrix elements (2.20)–(2.22), the shorthand definition

$$T_{b\gamma}(z)|d(-\mathbf{k}_\gamma)\rangle = \left[P_b + \sum_{a=N,\Delta} T_{ba}(z)\frac{P_a}{z-P_a[H_0+\delta H_0(z)]P_a} \right] \left[P_a + P_a H_1 Q \frac{Q}{z-QH_0Q} \right] H_1^\gamma P_N |d(-\mathbf{k}_\gamma)\rangle \quad (2.23)$$

is introduced—as discussed in Appendix A—providing also a computational advantage.

The derivation of cross sections from the matrix elements of the e.m. interaction (2.20)–(2.22) is standard for most reactions. Details are given in Refs. [5] and [6].

C. Parametrization of the hadronic and e.m. interactions

1. *Parametrization of the hadronic two-baryon interactions*

In isospin-triplet partial waves, the two-nucleon part $P_N H_1 P_N$ of the interaction Hamiltonian H_1 is chosen as

$$P_N H_1 P_N = V_{NN} - P_N H_1 P_\Delta \frac{P_\Delta}{2m_N c^2 - P_\Delta(H_0+H_1)P_\Delta} P_\Delta H_1 P_N \ . \quad (2.24)$$

The choice (2.24) yields approximate phase equivalence—at least at low energies—between the full coupled-channel force model and a realistic, but purely nucleonic reference potential V_{NN}. The Paris potential [17] is chosen as that reference potential V_{NN}. The prescription (2.24) employed is the same as in Refs. [1] and [3], though Ref. [1] considers a purely baryonic coupled-channel problem without pionic sector. Thus exact phase equivalence with the reference potential cannot be achieved even at zero kinetic energy, since the effective interaction of the full-force model in the two-nucleon channel, i.e.,

$$P_N \left[H_1 + H_1 P_\Delta \frac{P_\Delta}{z-P_\Delta[H_0+\delta H_0(z)+H_1+\delta H_1(z)]P_\Delta} P_\Delta H_1 \right] P_N = V_{NN} + P_N H_1 P_\Delta \left[\frac{P_\Delta}{z-P_\Delta[H_0+\delta H_0(z)+H_1+\delta H_1(z)]P_\Delta} - \frac{P_\Delta}{2m_N c^2 - P_\Delta(H_0+H_1)P_\Delta} \right] P_\Delta H_1 P_N \ , \quad (2.25)$$

does not coincide exactly with the reference potential V_{NN} at any energy z. In isospin-singlet partial waves, the two-nucleon part $P_N H_1 P_N$ of the interaction Hamiltonian H_1 is chosen to be identical with the reference potential V_{NN}.

The two-baryon transition potentials $P_\Delta H_1 P_N$ for Δ-isobar excitation and $P_N H_1 P_\Delta = (P_\Delta H_1 P_N)^+$ for Δ-isobar deexcitation are parametrized by π and ρ exchange, i.e.,

$$P_\Delta H_1 P_N = \sum_{\alpha=\pi,\rho} W_\alpha \ , \quad (2.26a)$$

with

$$\langle \mathbf{p}'_\Delta | W_\pi | \mathbf{p}_N \rangle = \frac{1}{(2\pi)^3}(-1)\frac{f_{\pi NN}}{m_\pi}\left[\frac{\Lambda_{\pi N}^2 - m_\pi^2}{\Lambda_{\pi N}^2 + (\mathbf{p}'_\Delta - \mathbf{p}_N)^2}\right]\frac{f_{\pi N\Delta}}{m_\pi}\left[\frac{\Lambda_{\pi\Delta}^2 - m_\pi^2}{\Lambda_{\pi\Delta}^2 + (\mathbf{p}'_\Delta - \mathbf{p}_N)^2}\right]\tau(1)\cdot\tau_{\Delta N}(2)$$
$$\times\left[\frac{[\sigma(1)\cdot(\mathbf{p}'_\Delta - \mathbf{p}_N)][\sigma_{\Delta N}(2)\cdot(\mathbf{p}'_\Delta - \mathbf{p}_N)]}{m_\pi^2 + (\mathbf{p}'_\Delta - \mathbf{p}_N)^2} - \frac{1}{3}\sigma(1)\cdot\sigma_{\Delta N}(2)\right], \tag{2.26b}$$

$$\langle \mathbf{p}'_\Delta | W_\rho | \mathbf{p}_N \rangle = \frac{1}{(2\pi)^3}(-1)\frac{f_{\rho NN}}{m_\pi}\left[\frac{\Lambda_{\rho N}^2 - m_\rho^2}{\Lambda_{\rho N}^2 + (\mathbf{p}'_\Delta - \mathbf{p}_N)^2}\right]\frac{f_{\rho N\Delta}}{m_\pi}\left[\frac{\Lambda_{\rho\Delta}^2 - m_\rho^2}{\Lambda_{\rho\Delta}^2 + (\mathbf{p}'_\Delta - \mathbf{p}_N)^2}\right]\tau(1)\cdot\tau_{\Delta N}(2)$$
$$\times\left[\frac{[\sigma(1)\times(\mathbf{p}'_\Delta - \mathbf{p}_N)][\sigma_{\Delta N}(2)\times(\mathbf{p}'_\Delta - \mathbf{p}_N)]}{m_\rho^2 + (\mathbf{p}'_\Delta - \mathbf{p}_N)^2} - \frac{2}{3}\sigma(1)\cdot\sigma_{\Delta N}(2)\right]. \tag{2.26c}$$

The operators $\sigma_{\Delta N}$ ($\tau_{\Delta N}$) are the transition spin (isospin) operators from a nucleon to a Δ isobar. The employed meson parameters are listed in Table I. They are taken from Refs. [18] and [19]. In contrast to Ref. [3], a monopole form factor is used. Furthermore, the δ-function contributions to the unregularized forms of the potential are removed by the terms proportional to $\sigma(1)\cdot\sigma_{\Delta N}(2)$.

The potential $P_\Delta H_1 P_\Delta$ in the nucleon-Δ channel consists of a direct and an exchange part according to processes (d) and (c) of Fig. 1. Both parts are parametrized by meson exchange as for the force model A3 of Ref. [1] with one distinction: In contrast to Ref. [1], one time ordering of the pion-mediated exchange part with pion–two-nucleon intermediate states is generated by the $\pi N\Delta$ vertex as a reducible process. Only the time ordering with pion–two-Δ intermediate states is contained in $P_\Delta H_1 P_\Delta$, corresponding to Fig. 1(c), and it is parametrized as in Ref. [3], distinct from the one in Ref. [1] with respect to the regularizing cutoff. The employed meson parameters are listed in Table II. They are taken from Ref. [20], a slight, but inconsequential change compared with Ref. [1]. In contrast, Refs. [21–23] choose the nucleon-Δ interaction differently. Whereas Refs. [21] and [23] parametrize a separable nucleon-Δ transition matrix, only Ref. [22] defines an instantaneous potential $P_\Delta H_1 P_\Delta$ for a consistent interaction Hamiltonian, though in Ref. [22] it is separable and nonvanishing only for partial waves of orbital angular momentum zero.

The coupling between baryonic and pionic channels is generated by the $\pi N\Delta$ vertex QH_1P_Δ of Fig. 1(e). It yields a pion-mediated retarded-exchange contribution to the nucleon-Δ interaction, and it yields the dressing (2.1) of the Δ propagator. The parametrization of the vertex QH_1P_Δ is the same as in Ref. [3].

2. *Parametrization of the e.m. current*

The parametrization of the e.m. interaction H^γ_I is taken from Refs. [5] and [6]. The external e.m. $A^\mu(\mathbf{x})$ is employed in Coulomb gauge, i.e., $A^\mu(\mathbf{x})=(0, \mathbf{A}(\mathbf{x}))$. Thus H^γ_I couples the photon exclusively to the spatial part $\mathbf{j}(\mathbf{x})$ of the hadronic current $j^\mu(\mathbf{x})=(\rho(\mathbf{x}), \mathbf{j}(\mathbf{x}))$. In the present calculation, we only take contributions from the nonrelativistic baryon currents $P_N\mathbf{j}(\mathbf{x})P_N$ and $P_\Delta\mathbf{j}(\mathbf{x})P_N$ into account. The e.m. current $P_N\mathbf{j}(\mathbf{x})P_N$ in the nucleonic Hilbert sector consists of the usual one- and two-nucleon pion-exchange currents. Their explicit forms are given in Refs. [5], [6], [24], and [25].

In the transition current $P_\Delta\mathbf{j}(\mathbf{x})P_N$ connecting the hadronic Hilbert sectors $\mathcal{H}_N$ and $\mathcal{H}_\Delta$, only the one-body current $P_\Delta\mathbf{j}^{[1]}(\mathbf{x})P_N$ is included in the present calculation. It is approximated by its dominant magnetic dipole part, while the electric quadrupole transition is neglected. Its explicit form is given in Refs. [5] and [6].

D. Calculational procedure

The various versions of the integral equations considered in practical calculations and the numerical method of their solution by cubic splines are described in Appendix A. Partial-wave expansions are used for the hadronic potentials and transition matrices and for the e.m. interaction. The expansion includes partial waves up to total angular momentum $J=6$. For the instantaneous potential $P_\Delta H_1 P_\Delta$ in the nucleon-Δ channel and for the induced transition $P_\Delta H^\gamma_I P_N$ from two-nucleon to nucleon-Δ states, the partial waves with total angular momenta $J=5$ and 6 are found to make an unimportant contribution and are therefore left out.

The practical calculations of this paper are based on the full hadronic force model as parametrized in Sec. II C 1. The comparison with reference results, obtained when the full instantaneous potential $P_\Delta H_1 P_\Delta$ in the nucleon-Δ channel is reduced to the one of Ref. [3], will indicate the importance of that potential on the observ-

TABLE I. Parameters of the transition potential (2.26) from two-nucleon to nucleon-delta states.

α	$f^2_{\alpha NN}/4\pi$	$f^2_{\alpha N\Delta}/4\pi$	$\Lambda_{\alpha N}$ (MeV)	$\Lambda_{\alpha\Delta}$ (MeV)
π	0.08	0.35	650	650
ρ	3.21	9.13	650	650

TABLE II. Meson parameters employed in the instantaneous nucleon-Δ potential.

α	$g^2_\alpha/4\pi$	k_α	m_α (MeV)	Λ_α (GeV)
π	14.4		138	1.2
σ	5.7		550	1.2
ρ	0.55	6.6	760	1.2
ω	20.0	0	783	1.2

ables of the studied reactions. Furthermore, the reference results yield the first recalculation of results of Ref. [3], which are found to be erroneous [26] to some extent.

When comparing with experimental data, the theoretical cross sections are used in a fully relativistic form. In contrast, the on-shell transition-matrix elements $U(z)$, required for the cross sections, are obtained from computations with nonrelativistic kinematics for baryons and with relativistic kinematics for the pion. Thus the identification between the fully relativistic experimental and half-relativistic calculational kinematics is not unique. In this paper all on-shell momenta and all available energies are derived from the fully relativistic experimental kinematics. Thus the transition-matrix elements resulting from that procedure are not strictly on their energy shell with respect to the half-relativistic calculational kinematics.

III. RESULTS

The results are discussed separately for the different reactions studied. Sections III A–III E consider the hadronic reactions, and Secs. III F and III G consider photon reactions.

The study of those reactions aims to single out the observables which are more sensitive to the instantaneous $N\Delta$ interaction. Those will be the most appropriate for extensive theoretical and experimental study, if one wants to gain a more complete understanding of the $N\Delta$ potential. (In Figs. 3–14 and 17–21, the dashed lines refer to the results of the reference force model [3,18] without the full $N\Delta$ potential $P_\Delta H_1 P_\Delta$ and the solid lines refer to the results obtained with that $N\Delta$ potential.)

A. Elastic two-nucleon scattering

Figures 3–7 show the effect of the instantaneous $N\Delta$ potential on the NN phase shifts and inelasticities for several uncoupled partial waves. At laboratory energies below 300 MeV, both curves are very similar to those of the Paris potential as a result of prescription (2.24), which guarantees approximate phase equivalence. Phase shifts and inelasticities below 300 MeV are therefore not shown. The biggest changes due to the $N\Delta$ potential are observed for the inelasticities of the $^3P_0$ and $^1D_2$ partial waves. In the first case, the $N\Delta$ potential yields an increase of the inelasticity, improving the agreement with the experimental data. In the second case, the effect is opposite; i.e., the inelasticity decreases, enhancing the deviation from the data. That behavior is due to partial-wave coupling in the $N\Delta$ sector: The $N\Delta$ potential couples strongly the $N\Delta$ $^5S_2$ and $^5D_2$ partial waves, removing flux from the S wave to the D wave. Thus the two-nucleon $^1D_2$ inelasticity decreases, since the coupled $N\Delta$ $^5S_2$ partial wave is suppressed. We conclude that the complete effect of the instantaneous $N\Delta$ potential cannot be simulated by its S wave alone.

The total inelasticity generated by our model, without the inclusion of the $N\Delta$ potential, is below the data. Moreover, the $N\Delta$ potential lower even more the inelasticity, at 800 MeV. This indicates that the NN-$N\Delta$ transition potential needs to be readjusted. However, for the purpose of a study of the effects of the $N\Delta$ potential, we think that the present limited model is sufficient.

It has been known for quite some time [15] that most existing models, based on a three-body NN-$N\Delta$-πNN formalism, are able to reproduce reasonably well the inelasticity in spin-singlet states, but invariably underestimate it for the spin-triplet states. It is therefore interesting to study the effect of the $N\Delta$ potential on the spin-singlet and -triplet components of the inelastic cross sections $pp \to \pi NN$ and $pp \to \pi^+ d$. The results of this comparison are shown in Tables III and IV for the two energies 578 and 800 MeV. The ratio σ_1/σ_0 of the spin-triplet to -singlet inelastic cross sections is underestimated by the

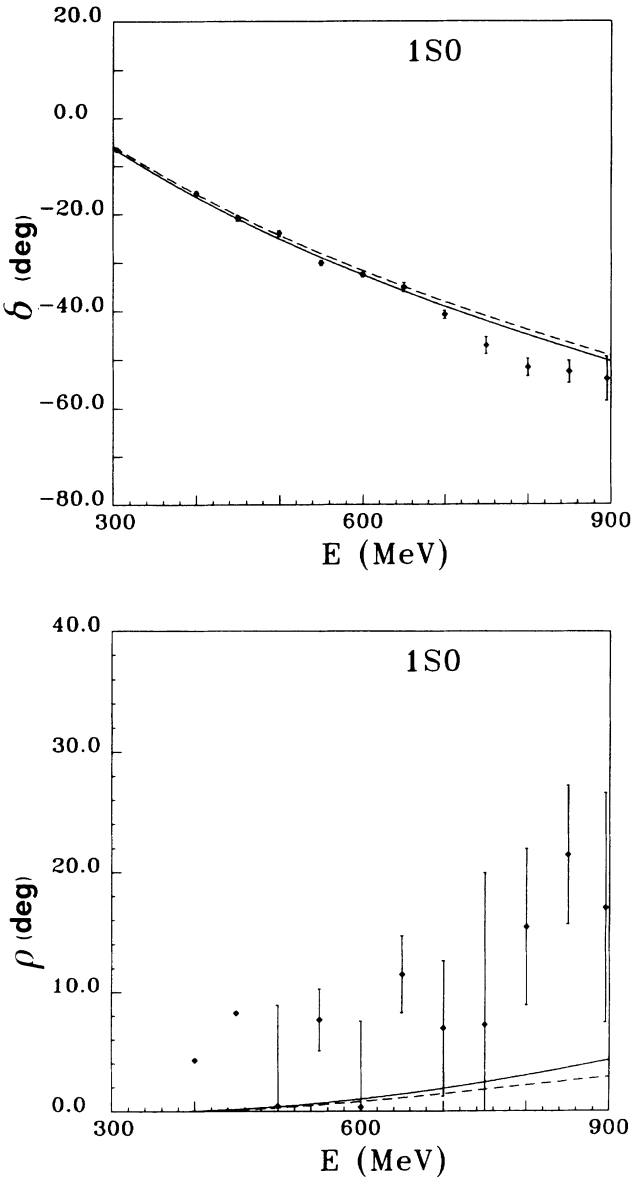

FIG. 3. Nucleon-nucleon scattering parameters δ and ρ for the $^1S_0$ partial wave as a function of proton laboratory energy. Solid (dashed) lines are the results with (without) the instantaneous $N\Delta$ potential. Data are from Ref. [27].

TABLE III. Spin decomposition of the inelastic reaction $pp \rightarrow \pi NN$. The experimental values were obtained using the analysis of Refs. [27] and [28].

	578 MeV σ_1 (mb)	σ_0 (mb)	σ_1/σ_0
Without $N\Delta$ potential	1.7	2.6	0.66
With $N\Delta$ potential	4.0	2.9	1.40
Experiment	5.3	2.8	1.89
	800 MeV σ_1 (mb)	σ_0 (mb)	σ_1/σ_0
Without $N\Delta$ potential	7.6	5.2	1.46
With $N\Delta$ potential	8.6	2.9	2.97
Experiment	15.2	5.1	2.98

TABLE IV. Spin decomposition of the inelastic NN reaction $pp \rightarrow \pi^+ d$. The experimental values were obtained using the analysis of Ref. [28].

	578 MeV σ_1 (mb)	σ_0 (mb)	σ_1/σ_0
Without $N\Delta$ potential	0.30	1.67	0.18
With $N\Delta$ potential	0.62	2.29	0.27
Experiment	0.87	2.18	0.40
	800 MeV σ_1 (mb)	σ_0 (mb)	σ_1/σ_0
Without $N\Delta$ potential	0.43	0.95	0.45
With $N\Delta$ potential	0.53	0.24	2.21
Experiment	0.63	0.56	1.13

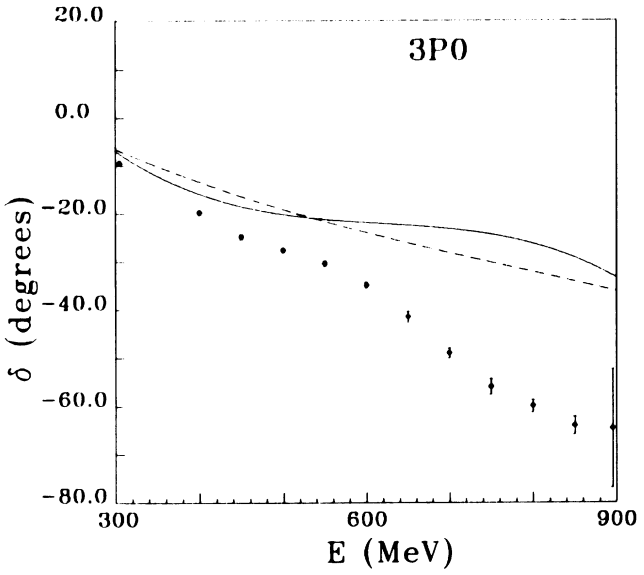

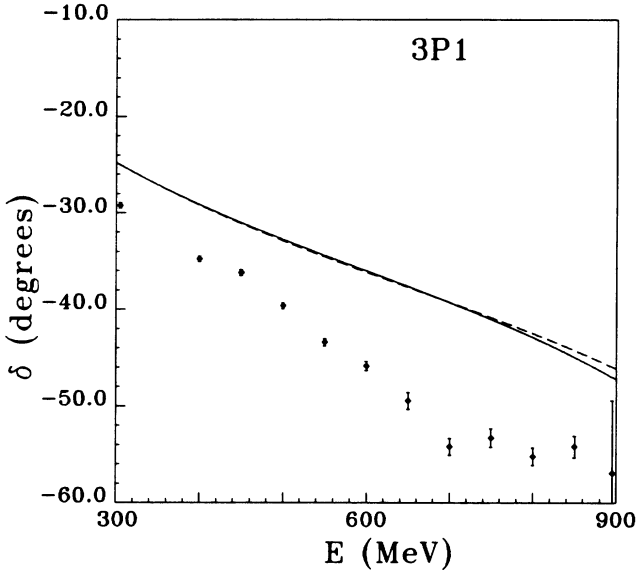

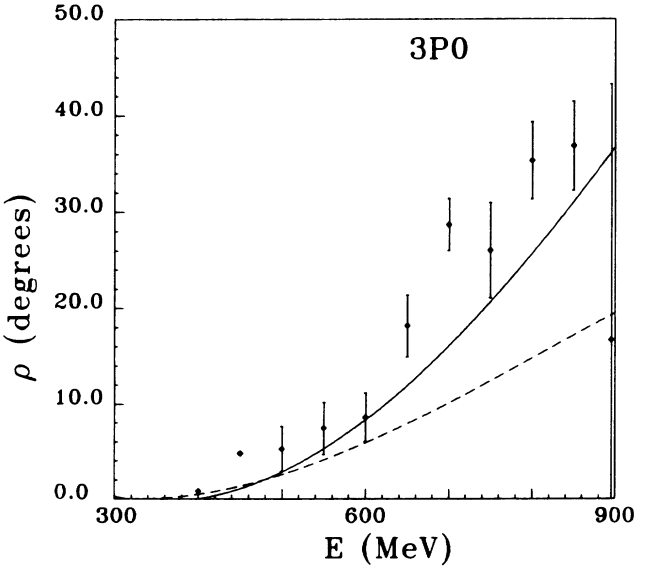

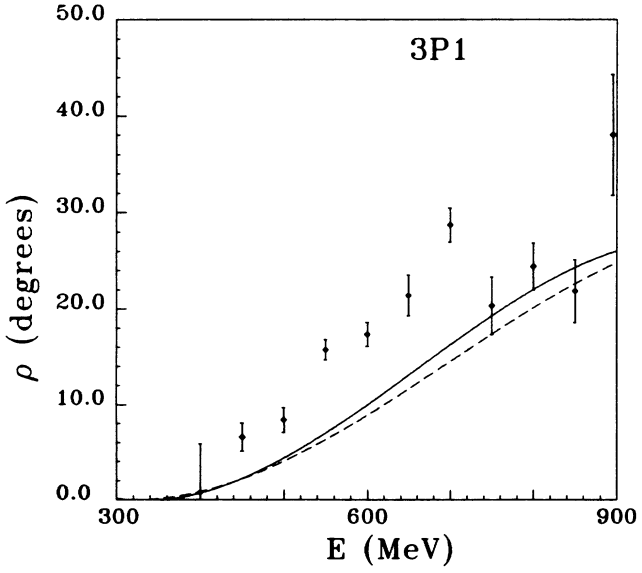

FIG. 4. Same as Fig. 3 for the $^3P_0$ partial wave.

FIG. 5. Same as Fig. 3 for the $^3P_1$ partial wave.

standard calculation without the $N\Delta$ potential. However, the $N\Delta$ interaction raises the ratio so as to bring it closer to the experimental value. In the case of the reaction $pp \rightarrow \pi NN$ at 800 MeV, the individual cross sections are lower than the experimental ones, but nevertheless, the ratio σ_1/σ_0 is reproduced correctly upon introducing the $N\Delta$ potential, so that it is reasonable to expect that a satisfactory description of both cross sections will be obtained once a new readjustment of the NN-$N\Delta$ transition potentials has been carried out. In case of the reaction $pp \rightarrow \pi^+ d$ at 800 MeV, the inclusion of the instantaneous $N\Delta$ interaction actually increases the ratio σ_1/σ_0 too much. The relevant conclusion to draw is that the $N\Delta$ potential provides a mechanism to balance correctly the relative importance of the spin-singlet and -triplet inelastic strength, a feature that has been lacking in almost all known standard NN-$N\Delta$-πNN models.

B. Elastic pion-deuteron scattering

Results for the differential cross section and spin observables iT_{11}, T_{20}, and T_{21} are shown in Figs. 8 and 9 at two pion energies. The instantaneous $N\Delta$ potential enhances the differential cross section at all angles for the pion laboratory kinetic energy of 140 MeV, while it has the opposite effect for the higher energy of 256 MeV. The polarization variables show a particular sensitivity on the inclusion of the $N\Delta$ potential at higher energies and backward angles.

The results of the present calculation agree for the

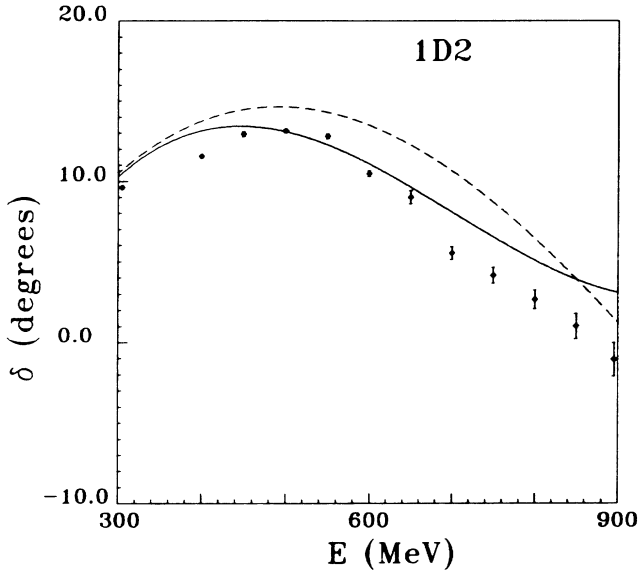

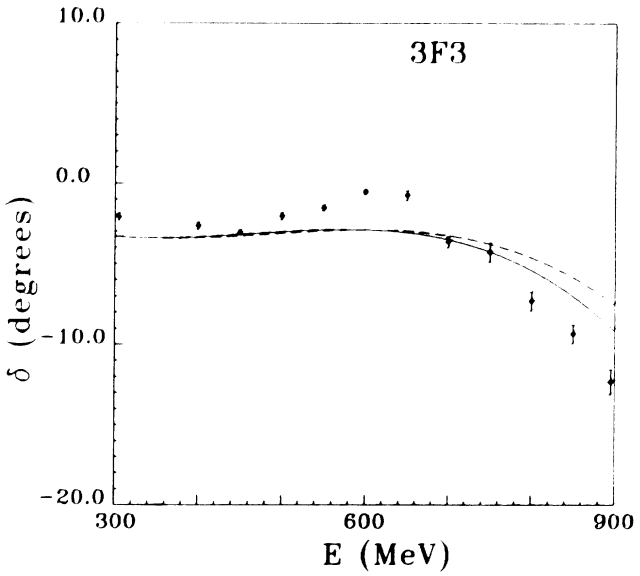

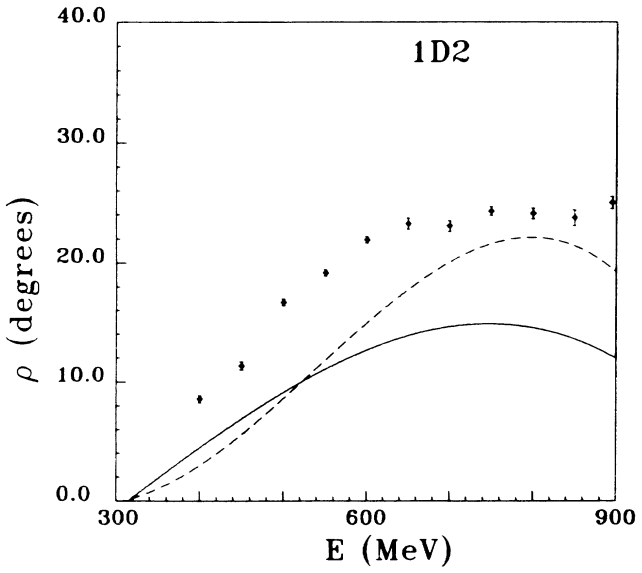

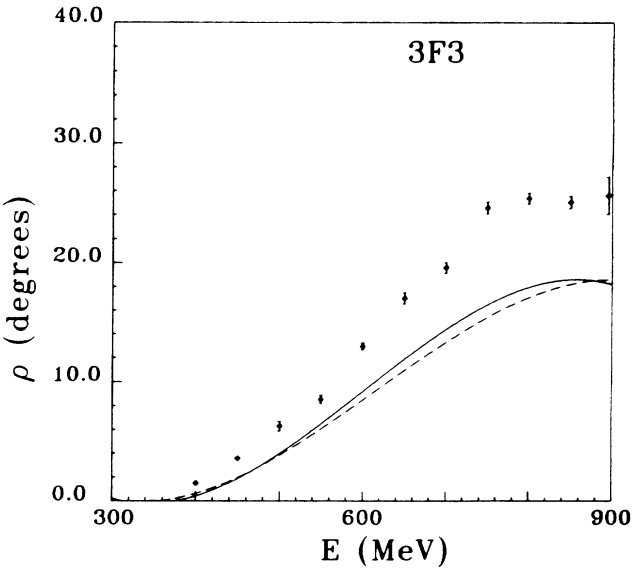

FIG. 6. Same as Fig. 3 for the $^1D_2$ partial wave.

FIG. 7. Same as Fig. 3 for the $^3F_3$ partial wave.

differential cross section qualitatively with those predicted by Alexandrou and Blankleider [22]. They are at variance with respect to the spin observable iT_{11}; the other spin observables cannot be compared. Ferreira, Andrade, and Dosch [21] inferred the existence of a strong $N\Delta$ interaction from the discrepancies between their theoretical prediction for the differential cross section in elastic pion-deuteron scattering and the experimental data. However, their analysis, extremely stimulating for the subsequent interest in the $N\Delta$ interaction, is based on Born approximation, presumably the reason why their predicted differential cross sections show a different energy dependence compared with the full calculations of Ref. [22] and of this paper.

Actually, also the work of Ref. [23], where one goes beyond the simple Born approximation and a full calculation is performed, coincides with the results of our model and of Ref. [22], finding the same kind of energy dependence for the effect of the $N\Delta$ potential.

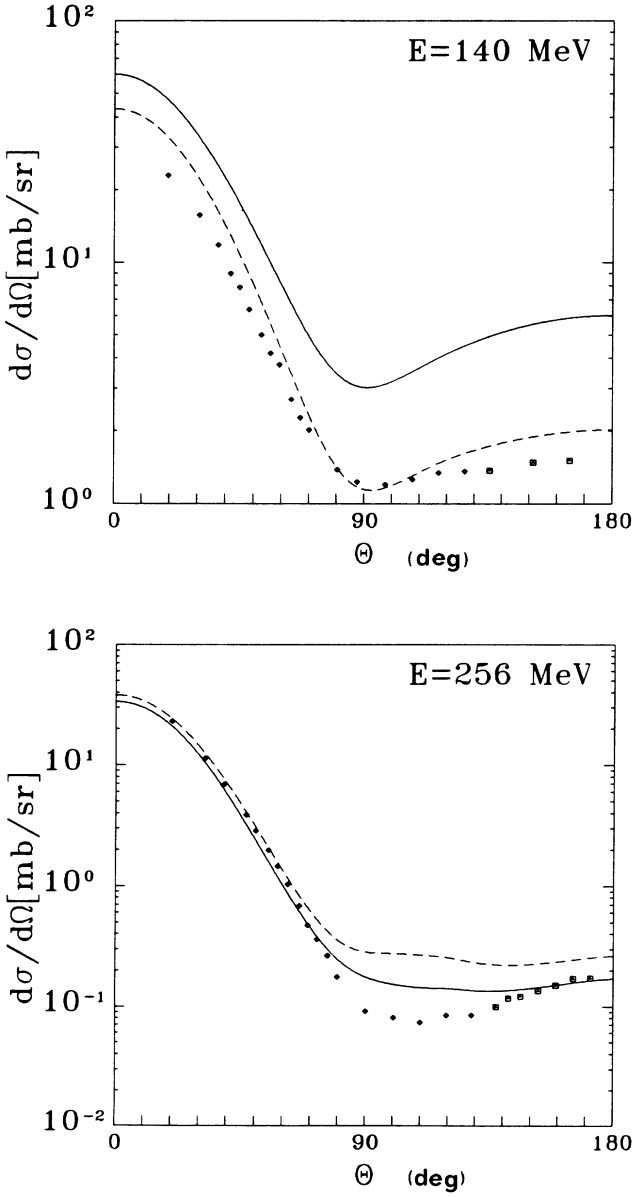

FIG. 8. $\pi d \to \pi d$ differential cross section $d\sigma/d\Omega$ at two pion laboratory energies. Solid (dashed) lines are the results with (without) the instantaneous $N\Delta$ potential. Data are from Refs. [29,30].

C. Reaction $NN \to \pi d$

This reaction is dominated by the contribution from the $NN\ ^1D_2$ partial wave, on which the instantaneous $N\Delta$ potential has a big effect according to Fig. 6 of Sec. III A. The results of Figs. 10–12 bear out the expected sensitivity: As in elastic pion-deuteron scattering, the differential cross section is increased at low energies and decreased at higher energies. The results of Alexandrou and Blankleider [22] show the same behavior.

The calculated polarization observables agree poorly with the experimental data. The inclusion of the instantaneous $N\Delta$ potential improves the agreement with data for A_{y0} at 800 MeV and especially A_{xx} and A_{yy} at 578 MeV. The calculated polarization observables also agree poorly with the results of Ref. [22]. The discrepancies exist, however, already for the respective reference force models without $N\Delta$ potential. Furthermore, the found effect of the $N\Delta$ potential is larger in the present calculation because of the inclusion of the $N\Delta\ ^5D_2$ partial wave.

D. Reaction $NN \to N\Delta\ (N\pi)$

The differential cross section and beam asymmetry A_y of the reaction $pp \to np\pi^+$ are displayed in Figs. 13 and 14, respectively, for the kinematic regime in which the proton and pion form a Δ^{++} resonance. The theoretical predictions are based on Eq. (B10). They are quite sensitive to the inclusion of the instantaneous $N\Delta$ potential. As for the differential cross section, the results obtained are below the data of Wicklund *et al.* [2], revealing the lack of inelastic strength that generally characterizes the model, as discussed in Sec. III A. However, previous calculations are not more successful in its agreement with data: Auger, Lazard, and Lombard [36] cannot reproduce the experimental differential cross section; Fayard *et al.* [37] cannot reproduce the experimental beam asymmetry. Furthermore, the calculation of Ref. [36] is less microscopic than the present one, since the ρ exchange in the transition potential to $N\Delta$ states carries an adjustable phase.

Reference [16] describes the transition amplitude to the particular $NN\pi$ states in which a Δ resonance is formed, approximately by effective $N\Delta$ phase shifts. The concept of Ref. [16] was developed for the single $N\Delta$ partial waves $^5S_2$ and $^5P_2$. Here it is generalized to an arbitrary number of $N\Delta$ partial waves and proven to be successful for the example of the differential cross section in Fig. 15 and for the beam asymmetry A_y in Fig. 16.

E. Reaction $\pi d \to N\Delta\ (N\pi)$

The result for the differential cross section of the reaction is shown in Fig. 17 for a pion incident laboratory en-

ergy of 256 MeV. The instantaneous $N\Delta$ potential lowers the cross section at almost all angles. This result agrees with other calculations [23,38]. In fact, Ref. [23] demonstrates that for the kinematically complete process $\pi^+ d \to \pi^+ np$ the main effect of the $N\Delta$ interaction is in general to lower the cross section, if the effect of the nucleon-nucleon final-state interaction is not included.

F. Reaction $\gamma d \to NN$

The results are shown in Figs. 18 and 19. The polarization observables T_{11}, T_{21}, and T_{22} are used in the definition of Ref. [44], which are twice those of the standard definition, as employed in Fig. 9 for elastic pion-deuteron scattering. The instantaneous $N\Delta$ potential

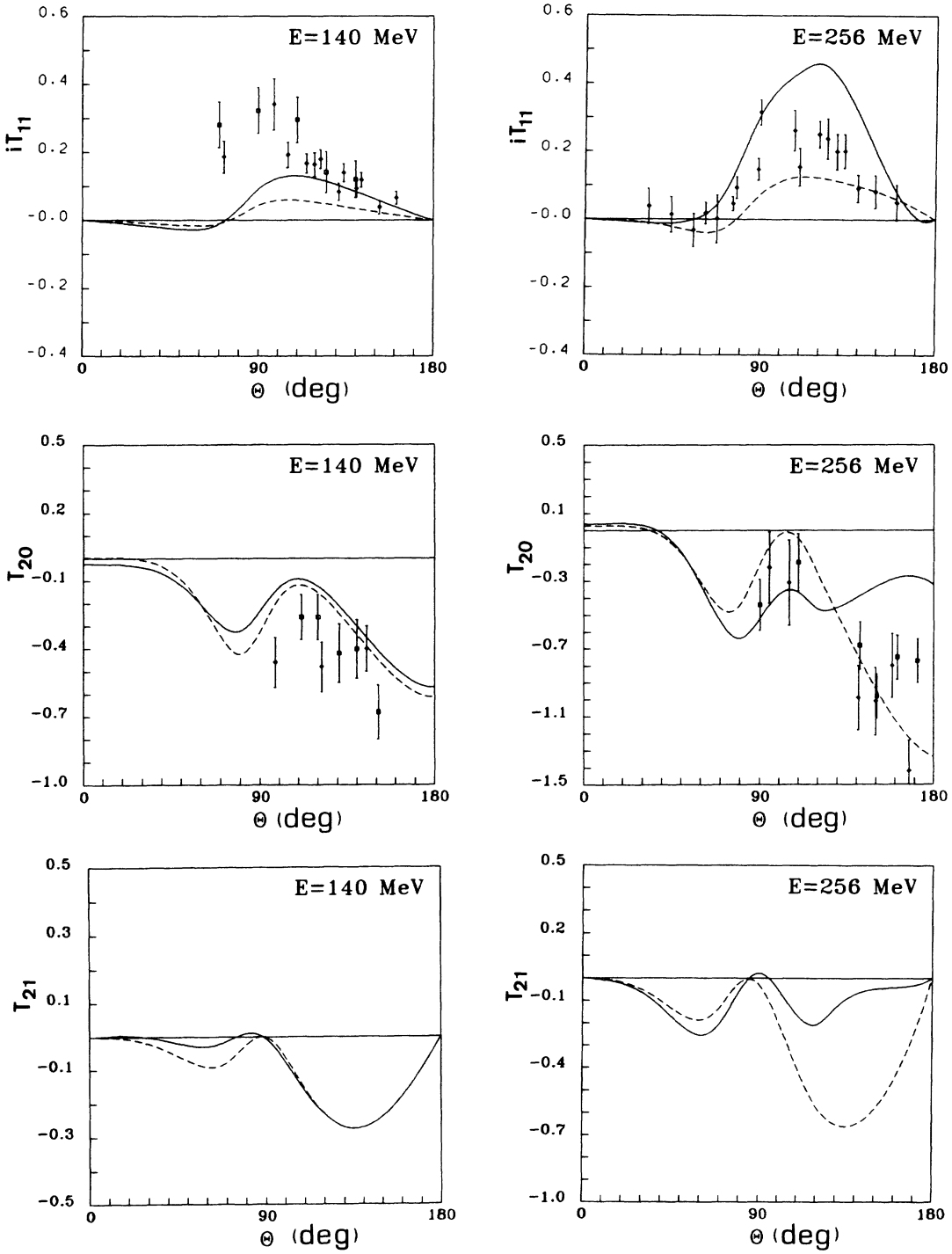

FIG. 9. Polarization observables iT_{11}, T_{20}, and T_{21} for the $\pi d \to \pi d$ reaction at the two pion laboratory energies of 140 and 256 MeV. Solid (dashed) lines are the results with (without) the instantaneous $N\Delta$ potential. Data from Refs. [31–33].

raises the differential cross section slightly. The photon asymmetry Σ seems to be somewhat improved. The deuteron analyzing powers exhibit little sensitivity, as shown by the examples of T_{11} and T_{22}, in contrast to the strong sensitivity of the proton asymmetry P_y.

G. Reaction $\gamma d \rightarrow \pi d$

The results are shown in Figs. 20 and 21. The polarization observables are defined again as in Ref. [44], differing from the standard definition. The largest effect of the instantaneous $N\Delta$ potential is seen in the differential cross section worsening the agreement with data. The present lack of experimental results for spin observables does not allow any further conclusions.

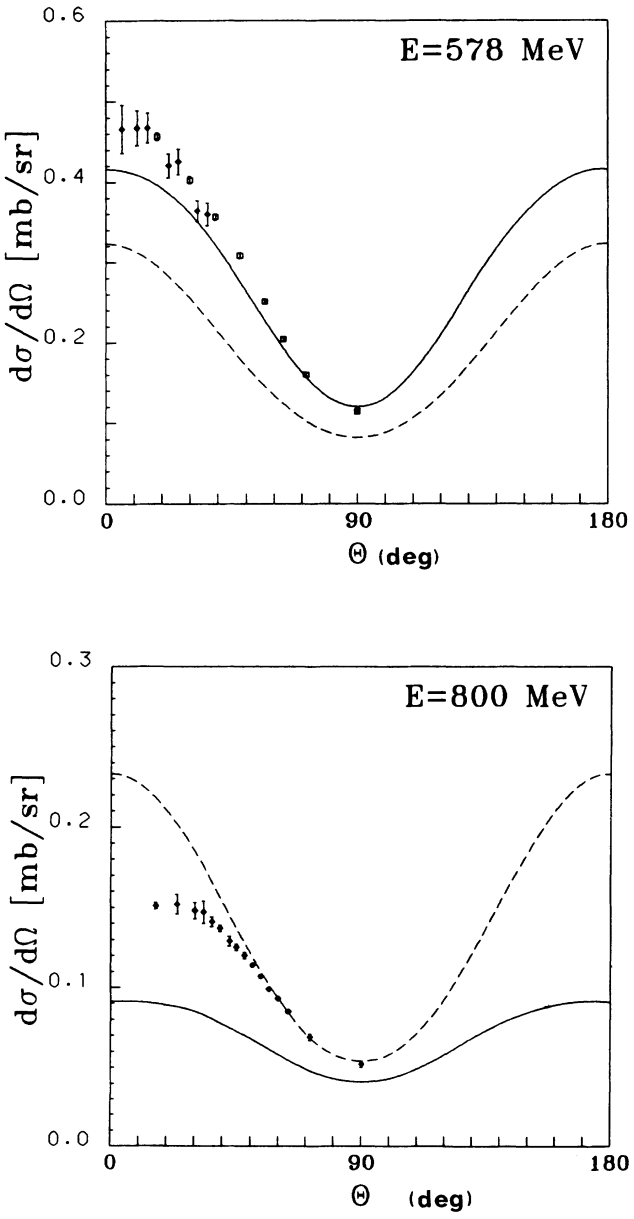

FIG. 10. Same as Fig. 8 for the reaction $NN \rightarrow \pi d$ at the two proton laboratory energies of 578 and 800 MeV. Data are taken from the compilation of Ref. [34].

IV. CONCLUSIONS

This paper considers the coupled two-nucleon and nucleon-Δ systems. They are used to study various reactions connecting the two-nucleon, pion-deuteron, photon-deuteron, and the three-body pion–two-nucleon channels. The effect of the instantaneous $N\Delta$ potential, parametrized in terms of meson exchanges, on observables of those reactions is investigated. Special sensitivities are found in the two-nucleon inelasticities of the $^3P_0$ and $^1D_2$ partial waves, in the differential cross section of elastic pion-deuteron scattering, in the differential cross section and spin observables of pion production with pion-deuteron and pion–two-nucleon final states, in the proton asymmetry of the deuteron photodisintegration, and in the differential cross section of the reaction $\gamma d \rightarrow \pi d$. As a general behavior, we find that for energies below the P_{33} resonance, the differential cross sections for the different reactions are raised by the inclusion of the $N\Delta$ potential, while the opposite effect occurs for the same observables at energies above the resonance. We also consider interesting that the instantaneous $N\Delta$ potential, which is not implicitly generated by the three-body models, is seen to provide the effect of balancing the inelastic strengths for nucleon-nucleon spin-triplet and -singlet states, enhancing the ratio of the two, a feature lacking so far in almost all existing standard models. Finally, we find most significant the effect of the $N\Delta$ instantaneous potential on the differential cross section and on the asymmetry parameter A_y of the pion-production reaction $pp \rightarrow n\Delta^{++}$ $(p\pi^+)$. However, despite those observed sensitivities, we cannot offer yet any practical procedure for determining parameters of the $N\Delta$ interaction.

Compared with the ground-breaking analysis of Ref. [21] and the calculation of Ref. [22] similar to ours, this paper employs a local instantaneous $N\Delta$ potential based on meson exchange, in contrast to Ref. [22], and takes it into account up to all required orders of scattering theory as Ref. [22] does. With respect to the reactions leading to pion–two-nucleon final states in the kinematic domain in which one nucleon and the pion form the P_{33} resonance, the full unapproximated scattering theory is also applied. However, it is checked that the approximative procedure of Ref. [16], which extracts effective $N\Delta$ phase shifts first and calculates then observables from them, is sufficiently accurate. Finally, the results obtained with the full $N\Delta$ potential $P_\Delta H_1 P_\Delta$ are compared to the results of the reference force model of Ref. [3]. Those reference results are the first recalculation of the predictions of Ref. [13] which are erroneous to some extent [26].

ACKNOWLEDGMENTS

We thank T. Mizutani for suggestions, in particular, for pointing out to us the possible importance of the $N\Delta$ potential in solving the unbalance problem between the two-nucleon spin-triplet and -singlet inelastic strengths. P.U.S. thanks the Nuclear Theory Group of the Universi-

ty of Washington for the kind hospitality extended to him during a stay there. The calculations for this paper were performed at "Regionales Rechenzentrum für Niedersachsen." This work was funded by the Deutsche Forschungs Gemeinschaft (DFG) under the Contract No. Sa 247/7-2, by the German Federal Minister for Research and Technology (BMFT) under the Contract No. 06OH752, by the German Academic Exchange Ser-

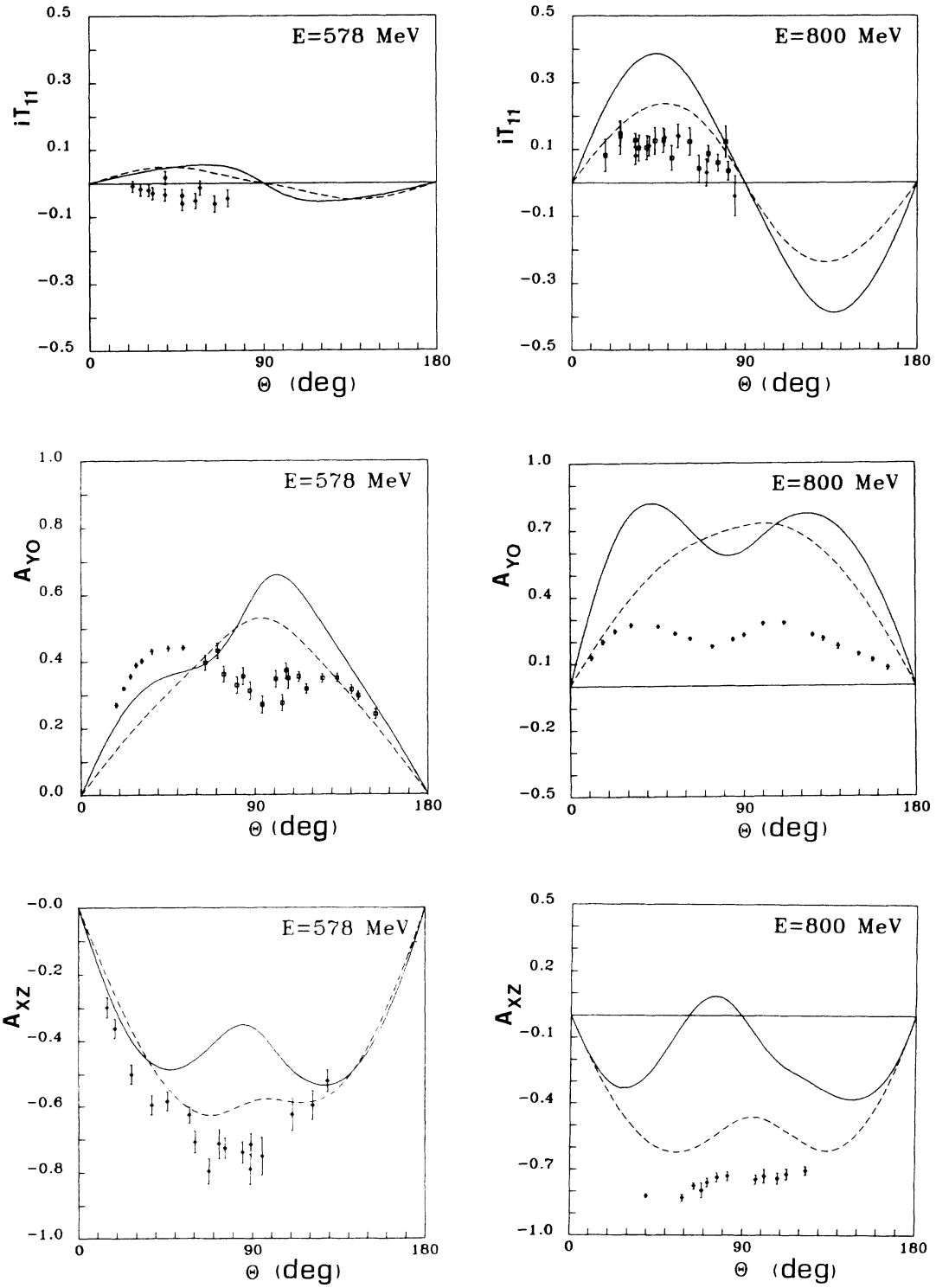

FIG. 11. Polarization observables iT_{11}, A_{y0}, and A_{xz} for the $NN \rightarrow \pi d$ reaction at the two proton laboratory energies of 578 and 800 MeV. Solid (dashed) lines are the results with (without) the instantaneous $N\Delta$ potential. Data are from Refs. [34,35].

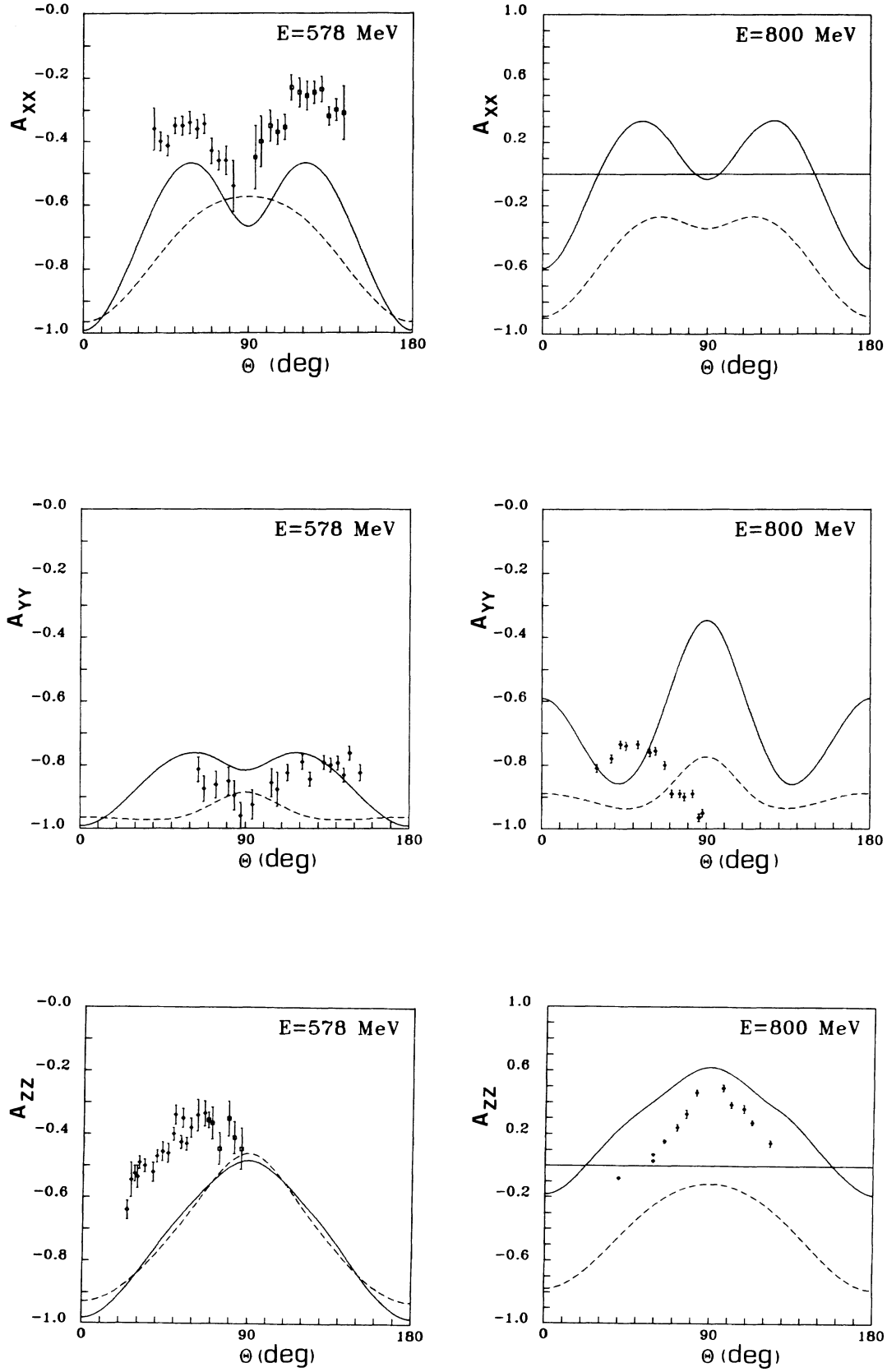

FIG. 12. Same as Fig. 11 for the polarization observables A_{xx}, A_{yy}, and A_{zz}. Data are from Ref. [34].

vice (DAAD) under the Contract No. 303-INIDA-dr and by the United States Department of Energy under the Contract No. DE-FG06-88ER40427.

APPENDIX A: COMPUTATIONAL PROCEDURES

1. Rearrangement of the integral equation (2.8) for the auxiliary transition matrix $T_{ba}(z)$

Using the notation

$$V_{ba}(z)=P_b[H_1+\delta H_1(z)]P_a \ , \tag{A1a}$$

$$G_a(z)=\frac{P_a}{z-P_a[H_0+\delta H_0(z)]P_a} \ , \tag{A1b}$$

the integral equation (2.8) takes the form

$$T_{ba}(z)=\sum_c V_{bc}(z)[\delta_{ca}+G_c(z)T_{ca}^{(z)}] \ . \tag{A2}$$

Within channel space, Eq. (A2) is a set of four equations which split into two groups of two coupled equations, i.e.,

$$T_{NN}(z)=V_{NN}+V_{NN}G_N(z)T_{NN}(z) + V_{N\Delta}G_\Delta(z)T_{\Delta N}(z) \ , \tag{A3a}$$

$$T_{\Delta N}(z)=V_{\Delta N}+V_{\Delta N}G_N(z)T_{NN}(z) + V_{\Delta\Delta}(z)G_\Delta(z)T_{\Delta N}(z) \ , \tag{A3b}$$

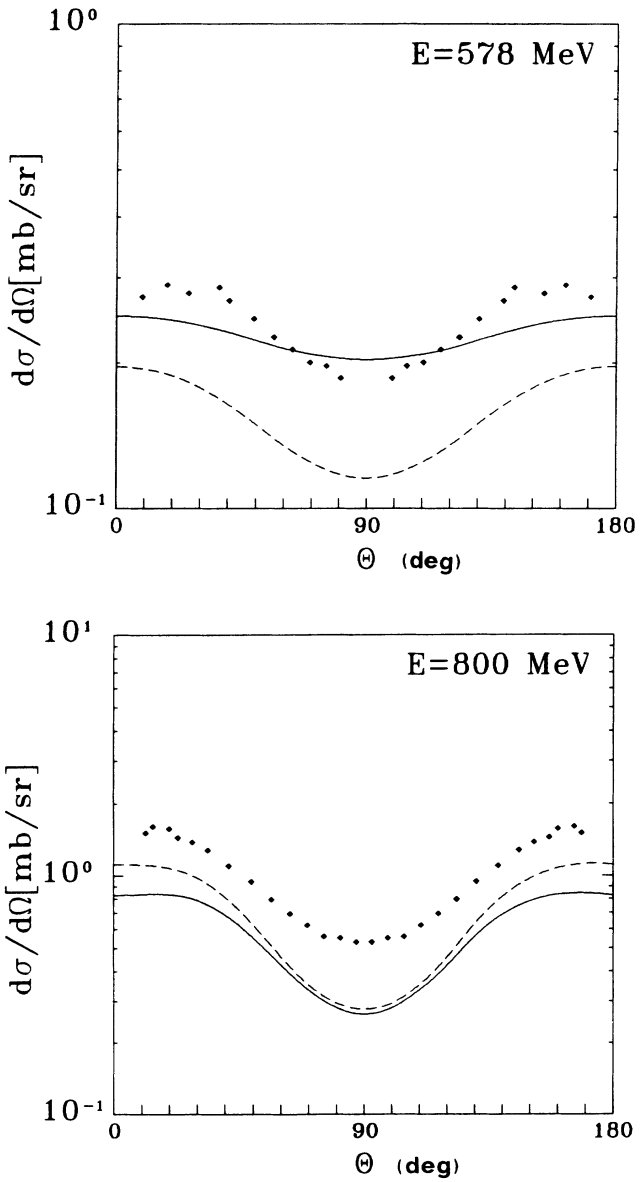

FIG. 13. Differential cross section $d\sigma/d\Omega$ for the reaction $pp\rightarrow n\Delta^{++}(p\pi^+)$ at incident proton energies of 578 and 800 MeV. Data are from Ref. [2]. Solid (dashed) curves are the results obtained with (without) the instantaneous $N\Delta$ potential.

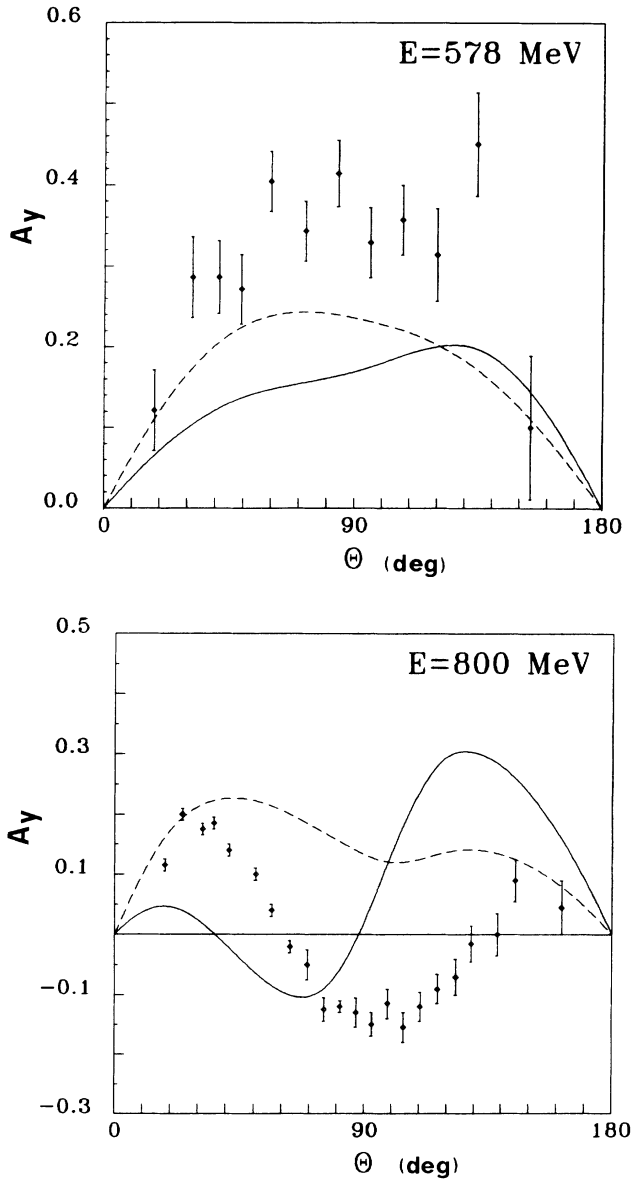

FIG. 14. Beam asymmetry A_y for the reaction $pp\rightarrow n\Delta^{++}(p\pi^+)$ at incident proton energies of 578 and 800 MeV. Data are from Ref. [2]. Solid (dashed) curves are the results obtained with (without) the instantaneous $N\Delta$ potential.

$$T_{N\Delta}(z)=V_{N\Delta}+V_{NN}G_N(z)T_{N\Delta}(z) + V_{N\Delta}G_\Delta(z)T_{\Delta\Delta}(z) , \quad \text{(A4a)}$$

$$T_{\Delta\Delta}(z)=V_{\Delta\Delta}(z)+V_{\Delta N}G_N(z)T_{N\Delta}(z) + V_{\Delta\Delta}(z)G_\Delta(z)T_{\Delta\Delta}(z) . \quad \text{(A4b)}$$

Only the interaction $V_{\Delta\Delta}(z)$ receives contributions from the eliminated pion channel and is dependent on the available energy z. The numerical solution of Eqs. (A3) and (A4) is simplified and its accuracy improved by eliminating the strong two-nucleon potential V_{NN} in favor of the smoother, purely nucleonic, and uncoupled transition matrix $t_{NN}(z)$, i.e.,

$$t_{NN}(z)=V_{NN}+V_{NN}G_N(z)t_{NN}(z) . \quad \text{(A5)}$$

Equations (A3) and (A4) then take the form

$$T_{NN}(z)=t_{NN}(z)+\tilde{V}_{N\Delta}(z)G_\Delta(z)T_{\Delta N}(z) , \quad \text{(A6a)}$$

$$T_{\Delta N}(z)=\tilde{V}_{\Delta N}(z)+\tilde{V}_{\Delta\Delta}(z)G_\Delta(z)T_{\Delta N}(z) , \quad \text{(A6b)}$$

$$T_{N\Delta}(z)=\tilde{V}_{N\Delta}(z)+\tilde{V}_{N\Delta}(z)G_\Delta(z)T_{\Delta\Delta}(z) , \quad \text{(A7a)}$$

$$T_{\Delta\Delta}(z)=\tilde{V}_{\Delta\Delta}(z)+\tilde{V}_{\Delta\Delta}(z)G_\Delta(z)T_{\Delta\Delta}(z) , \quad \text{(A7b)}$$

with the definitions

$$\tilde{V}_{N\Delta}(z)=[1+t_{NN}(z)G_N(z)]V_{N\Delta} , \quad \text{(A8a)}$$

$$\tilde{V}_{\Delta N}(z)=V_{\Delta N}[1+G_N(z)t_{NN}(z)] , \quad \text{(A8b)}$$

$$\tilde{V}_{\Delta\Delta}(z)=V_{\Delta\Delta}(z)+V_{\Delta N}G_N(z)\tilde{V}_{N\Delta}(z) . \quad \text{(A8c)}$$

The set of Eqs. (A6) and (A7) is used in practical calculations.

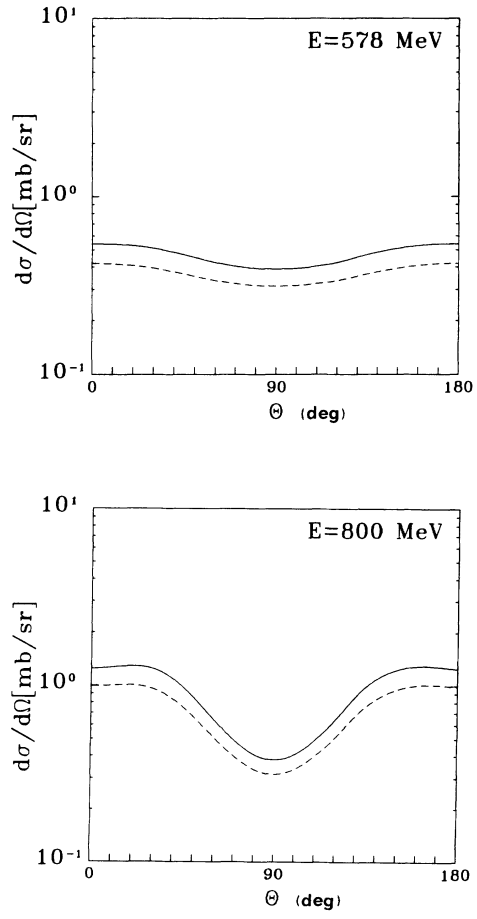

FIG. 15. Differential cross section $d\sigma/d\Omega$ for the reaction $pp\rightarrow n\Delta^{++}(p\pi^+)$. Solid curves are the exact results. Dashed curves are obtained from the approximation that consists in the averaging procedure introduced in Ref. [16].

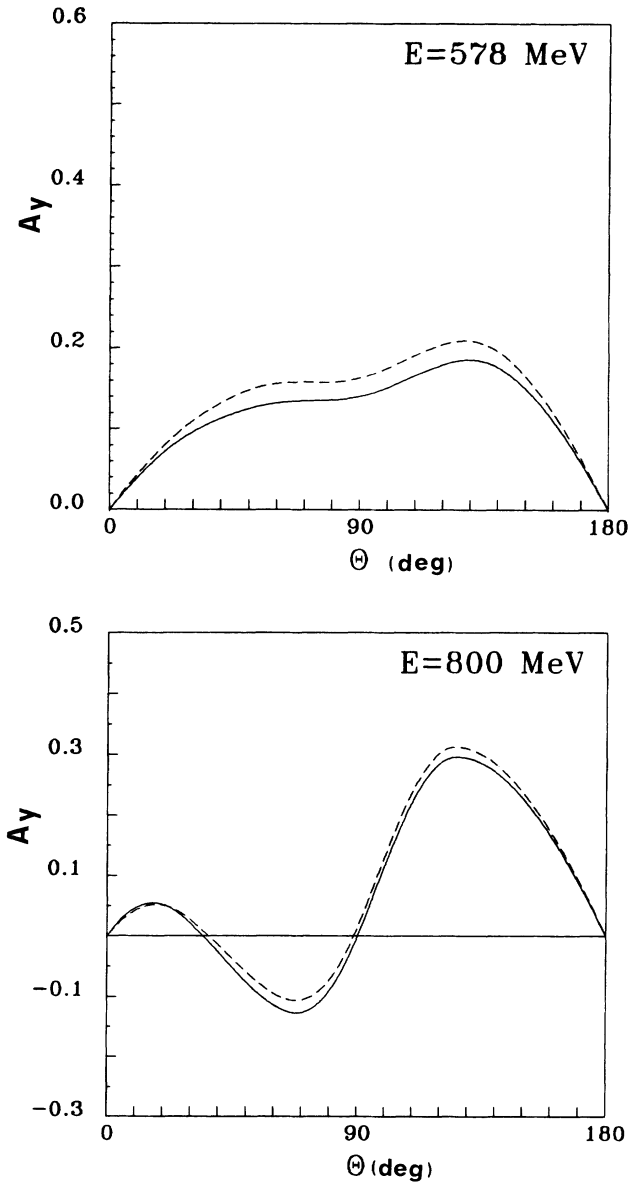

FIG. 16. Beam asymmetry A_y for the reaction $pp\rightarrow n\Delta^{++}(p\pi^+)$. Solid curves are the exact results. Dashed curves are obtained from the approximation that consists in the averaging procedure introduced in Ref. [16].

2. Calculation of the transition matrix (2.16c) for pion-deuteron channels

All scattering amplitudes (2.9)–(2.14) required for the description of the considered hadronic processes could be obtained from the integral equations (A6) and (A7). However, the on-shell scattering amplitudes $U_{N\pi}(z)$ and $U_{\pi\pi}(z)$ for pion-deuteron processes require completely off-shell elements of $T_{N\Delta}(z)$ and $T_{\Delta\Delta}(z)$. Thus it is advantageous to calculate the combination

$$T_{b\pi}(z)|\phi_\pi(\mathbf{q}_\pi)\rangle = \left[\delta_{b\Delta}+T_{b\Delta}(z)\frac{P_\Delta}{z-P_\Delta[H_0+\delta H_0(z)]P_\Delta}\right] \times P_\Delta H_1 Q|\phi_\pi(\mathbf{q}_\pi)\rangle \tag{A9}$$

directly and independently from $T_{NN}(z)$ and $T_{\Delta N}(z)$. Using the notation

$$V_{\Delta\pi}|\phi_\pi(\mathbf{q}_\pi)\rangle = P_\Delta H_1 Q|\phi_\pi(\mathbf{q}_\pi)\rangle \tag{A10}$$

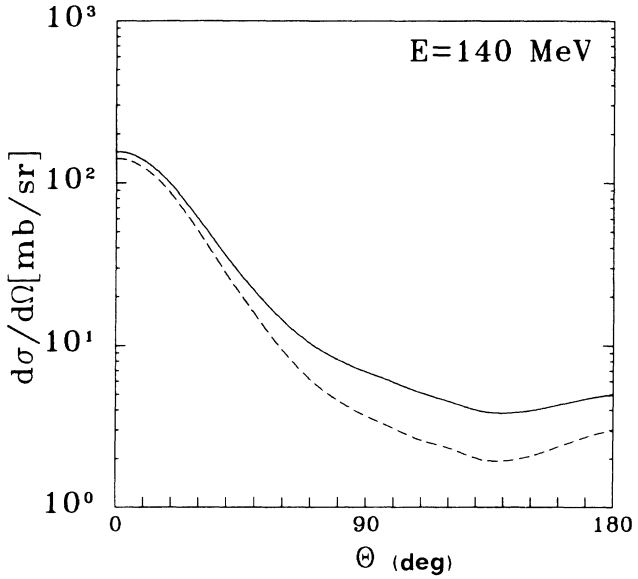

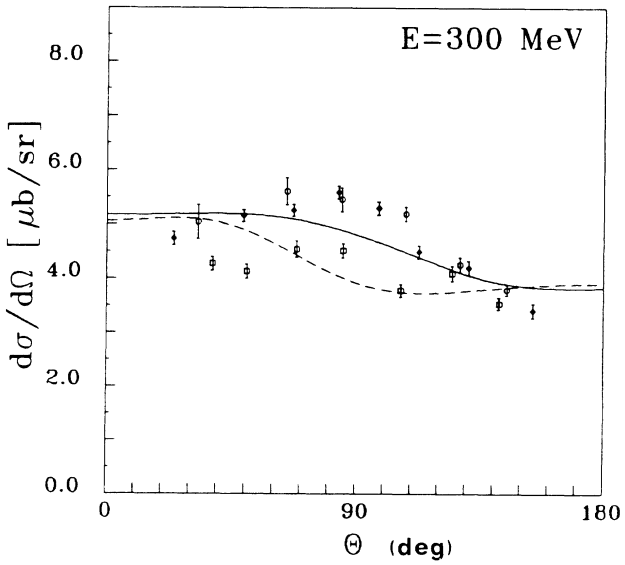

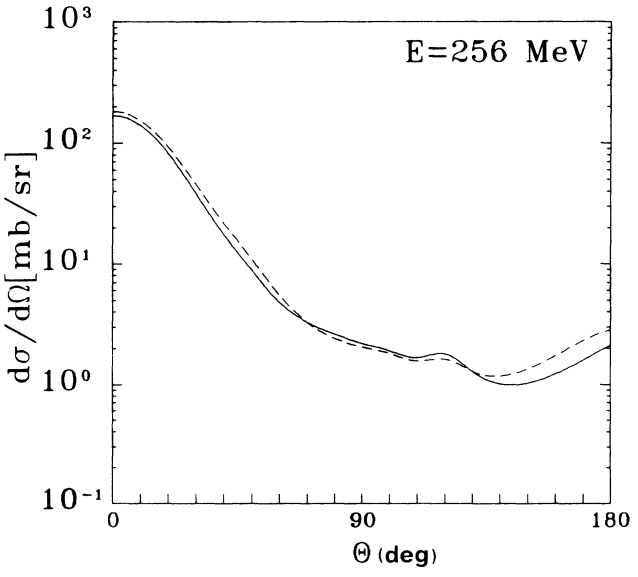

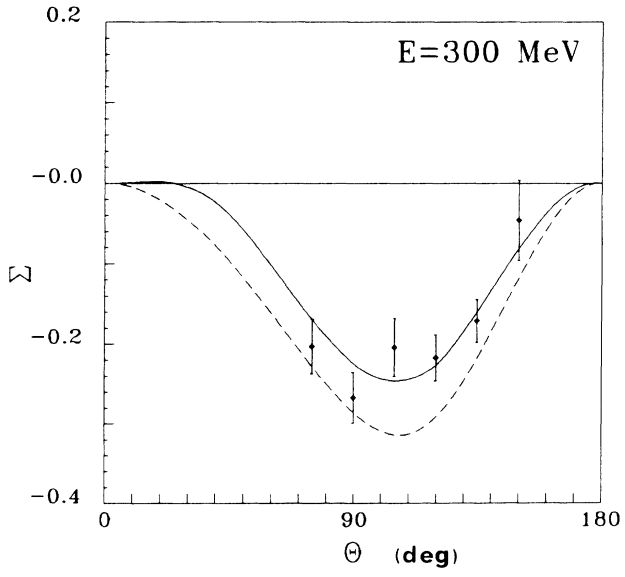

FIG. 17. Differential cross section $d\sigma/d\Omega$ for the reaction $\pi^+ d \to n\Delta^{++}(p\pi^+)$ at incident pion laboratory energies of 140 and 256 MeV. Solid (dashed) lines are the results with (without) the instantaneous $N\Delta$ potential.

FIG. 18. Differential cross section $d\sigma/d\Omega$ and photon asymmetry Σ for the reaction $\gamma d \to NN$ at an incident photon energy of 300 MeV. Solid (dashed) lines are the results with (without) the instantaneous $N\Delta$ potential. Data are from Refs. [39–43].

and Eq. (2.8), the following integral equation holds for $T_{b\pi}(z)$:

$$T_{b\pi}(z)=V_{b\pi}\delta_{\Delta b}+\sum_c V_{bc}(z)G_c(z)T_{c\pi}(z) \quad \text{(A11)}$$

or, explicitly,

$$T_{N\pi}(z)=V_{NN}G_N(z)T_{N\pi}(z)+V_{N\Delta}G_\Delta(z)T_{\Delta\pi}(z)\ , \quad \text{(A12a)}$$

$$T_{\Delta\pi}(z)=V_{\Delta\pi}+V_{\Delta N}G_N(z)T_{N\pi}(z)+V_{\Delta\Delta}(z)G_\Delta(z)T_{\Delta\pi}(z)\ . \quad \text{(A12b)}$$

Again, the latter integral equation is smoothened and consequently numerical accuracy gained by replacing the two-nucleon potential V_{NN} in favor of the transition matrix $t_{NN}(z)$ of Eq. (A5), i.e.,

$$T_{N\pi}(z)=\tilde{V}_{N\Delta}(z)G_\Delta(z)T_{\Delta\pi}(z)\ , \quad \text{(A13a)}$$

$$T_{\Delta\pi}(z)=V_{\Delta\pi}+\tilde{V}_{\Delta\Delta}(z)G_\Delta(z)T_{\Delta\pi}(z)\ . \quad \text{(A13b)}$$

The set (A13) of equations is used in practical calculations.

3. Calculation of the transition matrix (2.24b) for photon-deuteron channels

All scattering amplitudes $T_{ba}(z)$ required for the description (2.20)–(2.22) of the considered e.m. processes could be obtained from the integral equations (A6) and (A7). However, completely off-shell elements of $T_{ba}(z)$ are required. Thus it is advantageous to calculate the combination

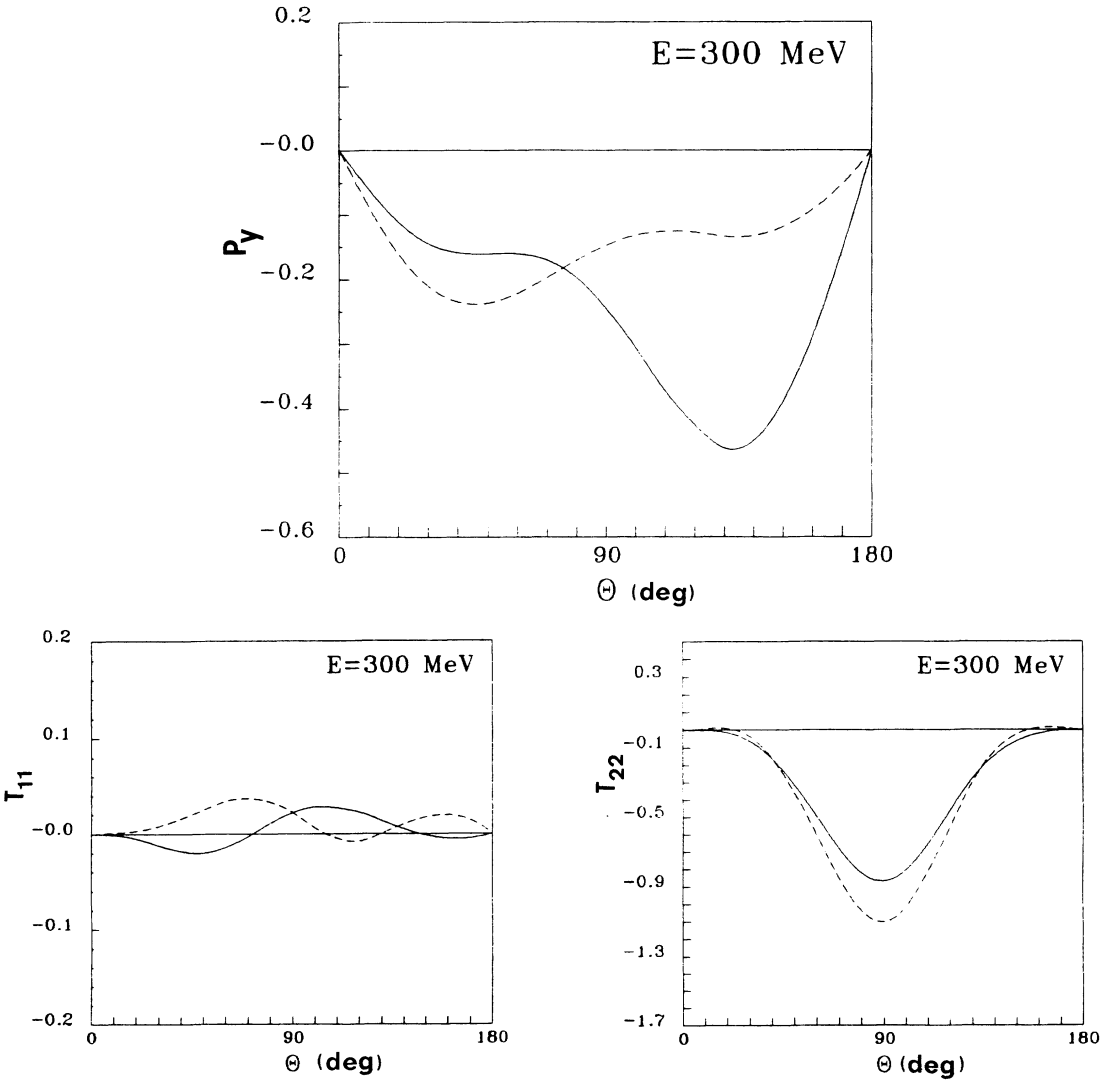

FIG. 19. Polarization observables P_y, T_{11}, and T_{22} for the reaction $\gamma d \rightarrow NN$ at an incident photon energy of 300 MeV. Solid (dashed) lines are the results with (without) the instantaneous $N\Delta$ potential.

$$T_{b\gamma}(z)|d(-\mathbf{k}_\gamma)\rangle = \left[P_b + \sum_{a=N,\Delta} T_{ba}(z)\frac{P_a}{z-P_a[H_0+\delta H_0(z)]P_a}\right] \times \left[P_a + P_a H_1 Q\frac{Q}{z-QH_0Q}\right] H_1^\gamma P_N|d(-\mathbf{k}_\gamma)\rangle \tag{A14}$$

directly and independently from $T_{ba}(z)$. Equation (A14) is a general definition. We note that the present calculation, however, does not take any channel coupling $QH_1^\gamma P_N$ into account. Using the notation

$$V_{b\gamma}(z)|d(-\mathbf{k}_\gamma)\rangle = \left[P_b + P_b H_1 Q\frac{Q}{z-QH_0Q}\right] H_1^\gamma P_N|d(-\mathbf{k}_\gamma)\rangle , \tag{A15}$$

the following integral equation holds for $T_{b\gamma}(z)$:

$$T_{b\gamma}(z) = V_{b\gamma}(z) + \sum_c V_{bc}(z)G_c(z)T_{c\gamma}(z) \tag{A16}$$

or, explicitly,

$$T_{N\gamma}(z) = V_{N\gamma}(z) + V_{NN}G_N(z)T_{N\gamma}(z) + V_{N\Delta}G_\Delta(z)T_{N\gamma}(z) , \tag{A17a}$$

$$T_{\Delta\gamma}(z) = V_{\Delta\gamma}(z) + V_{\Delta N}G_N(z)T_{N\gamma}(z) + V_{\Delta\Delta}(z)G_\Delta(z)T_{\Delta\gamma}(z) . \tag{A17b}$$

Again, the latter integral equation is smoothened by replacing the two-nucleon potential V_{NN} in favor of the transition matrix $t_{NN}(z)$ of Eq. (A5), i.e.,

$$T_{N\gamma}(z) = \tilde{V}_{N\gamma}(z) + \tilde{V}_{N\Delta}(z)G_\Delta(z)T_{\Delta\gamma}(z) , \tag{A18a}$$

$$T_{\Delta\gamma}(z) = \tilde{V}_{\Delta\gamma}(z) + \tilde{V}_{\Delta\Delta}(z)G_\Delta(z)T_{\Delta\gamma}(z) , \tag{A18b}$$

with the definitions

$$\tilde{V}_{N\gamma}(z) = [1 + t_{NN}(z)G_N(z)]V_{N\gamma} , \tag{A19a}$$

$$\tilde{V}_{\Delta\gamma}(z) = V_{\Delta\gamma}(z) + V_{\Delta N}G_N(z)\tilde{V}_{N\gamma}(z) . \tag{A19b}$$

The set (A18) of integral equations is used in practical calculations. The resulting operators $T_{N\gamma}(z)$ and $T_{\Delta\gamma}(z)$ allow a simplified computation of the hadronic currents (2.20)–(2.22).

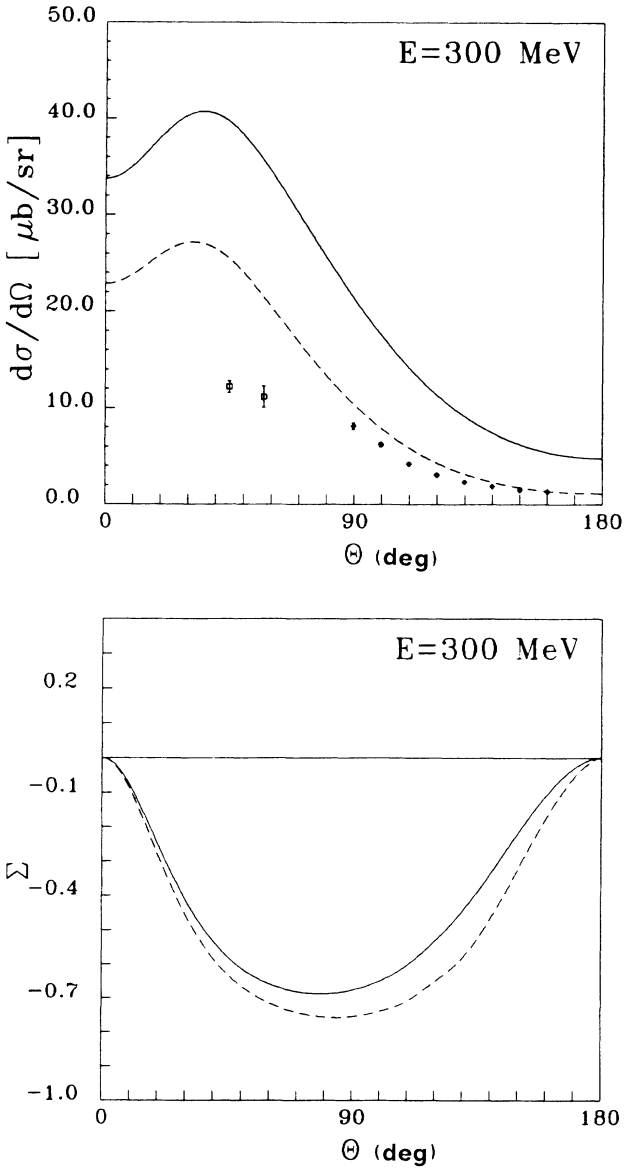

FIG. 20. Same as Fig. 18 for the reaction $\gamma d \to \pi^0 d$ at an incident photon energy of 300 MeV. Solid (dashed) lines are the results with (without) the instantaneous $N\Delta$ potential. Data are from Refs. [45,46].

4. Practical solution of the integral equations (A6b), (A7b), (A13b), and (A18b) using cubic splines

The integral equations (A6b), (A7b), (A13b), and (A18b) have the same kernels, differing only in their inhomogeneous terms.

Usually, one can solve those equations by matrix inversion. The three-body singularities arising in the $\tilde{V}_{\Delta\Delta}(z)$ potential can then be dealt with by the contour-rotation method. However, to deal with the breakup channels, one needs to have the transition matrices on the real axis. Once the contour-rotation method is used, difficulties are met to go back to the real axis. To avoid this problem, there are only two possible ways: the Padé-approximant or splines method. We have observed the failure of the Padé-approximant method to converge because of the strength of the nucleon-Δ instantaneous potential contained in the effective $\tilde{V}_{\Delta\Delta}(z)$ potential. This failure led us to choose the splines method already used in Refs. [47–49] in this and related contexts.

To solve the integral equations (A6b), (A7b), (A13b), and (A18b) of Appendixes A 1, A 2, and A 3, we made use of cubic Hermite splines [50,51]. Since all integral equations reduce to one master equation with the same kernel but different inhomogeneous terms, we exemplify here the procedure of practically solving all those equations by selecting Eq. (A6b).

In what follows we will use the partial-wave notation

$$T_{\Delta N}^{L_\Delta S_\Delta L_N S_N}(p_\Delta,p_N)=\langle p_\Delta(L_\Delta S_\Delta)\mathcal{J}T|T_{\Delta N}\left[2m_N c^2+\frac{p_N^2}{m_N}\right]|p_N(L_N S_N)\mathcal{J}T\rangle ,$$

for the half-shell transition matrix $T_{\Delta N}(z)$ and a corresponding one for the matrix elements of the $\tilde{V}_{\Delta N}(z)$ and $\tilde{V}_{\Delta\Delta}(z)$ potentials. The notation

$$g_\Delta(p_\Delta)|p_\Delta(L_\Delta S_\Delta)JT\rangle=G_\Delta\left[2m_N c^2+\frac{p_N^2}{m_N}\right]|p_\Delta(L_\Delta S_\Delta)JT\rangle$$

will also be used for the partial-wave Green's function. In the partial-wave notation, the quantum numbers $L_N(L_\Delta)$, $S_N(S_\Delta)$, $\mathcal{J}$, and T denote the orbital angular momentum, spin, total angular momentum, and isospin of the respective channels. The indices $\mathcal{J}$ and T are omitted in $T_{\Delta N}^{L_\Delta S_\Delta L_N S_N}(p_\Delta,p_N)$ since they are conserved and consequently the same in both sides of Eq. (A6b). After partial-wave decomposition, Eq. (A6b) reads

$$T_{\Delta N}^{L_\Delta S_\Delta L_N S_N}(p_\Delta,p_N)=\tilde{V}_{\Delta N}^{L_\Delta S_\Delta L_N S_N}(p_\Delta,p_N)+\sum_{L'_\Delta S'_\Delta}\int_0^\infty q'^2dq'\,\tilde{V}_{\Delta\Delta}^{L_\Delta S_\Delta L'_\Delta S'_\Delta}(p_\Delta,q')g_\Delta(q')T_{\Delta N}^{L'_\Delta S'_\Delta L_N S_N}(q',p_N) , \quad \text{(A20)}$$

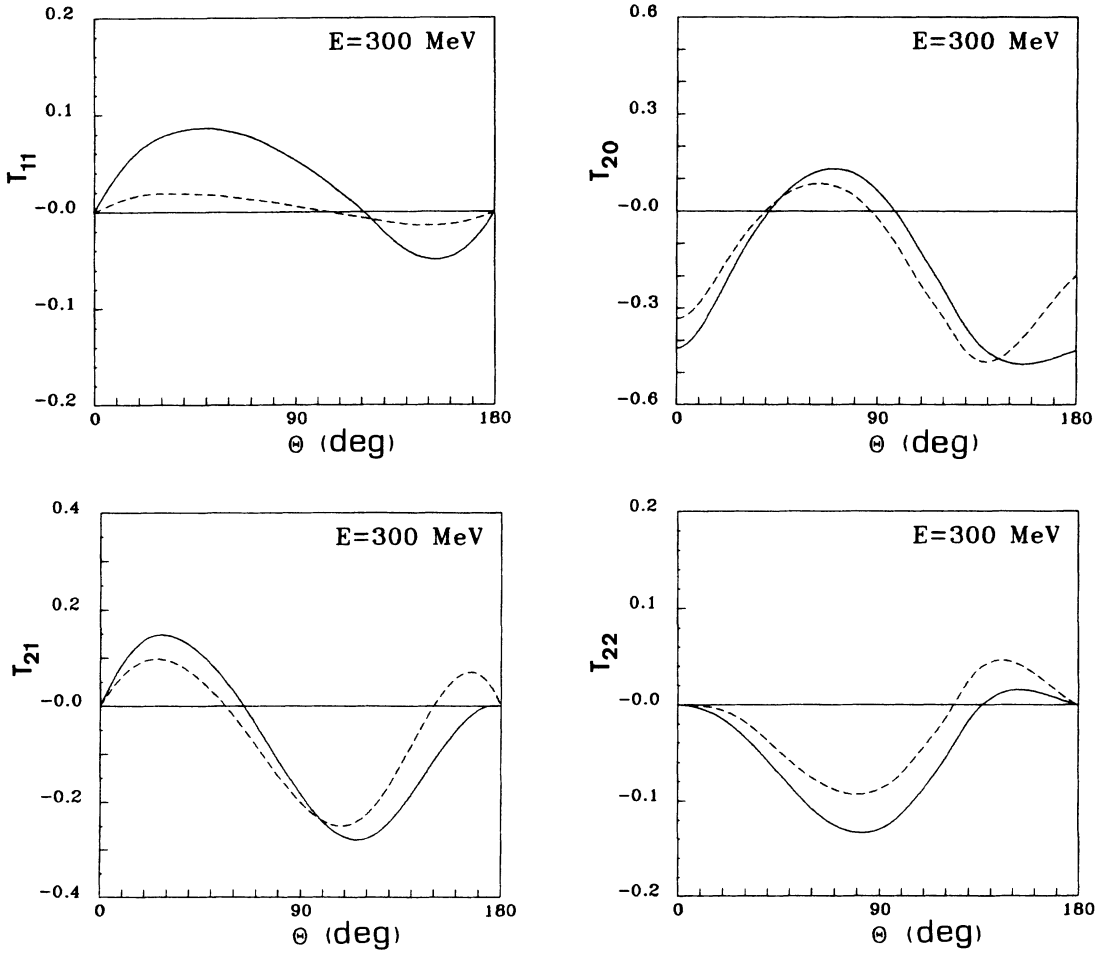

FIG. 21. Polarization observables T_{11}, T_{20}, T_{21}, and T_{22} for the reaction $\gamma d\rightarrow\pi^0 d$ at an incident photon energy of 300 MeV. Solid (dashed) lines are the results with (without) the instantaneous $N\Delta$ potential.

where p_N is the on-shell point. To handle correctly the boundary conditions, $T_{\Delta N}^{L_\Delta S_\Delta L_N S_N}(p_\Delta,p_N)\sim p_\Delta^{L_\Delta}=1$ at the origin for $L_\Delta=0$, we multiply (A20) by p_Δ. In this way we establish L_Δ-independent boundary conditions. Equation (A20) becomes

$$F_{\Delta N}^{L_\Delta S_\Delta L_N S_N}(p_\Delta,p_N)=p_\Delta \tilde{V}_{\Delta N}^{L_\Delta S_\Delta L_N S_N}(p_\Delta,p_N)+\sum_{L'_\Delta S'_\Delta}\int_0^\infty q'\,dq'\,p_\Delta \tilde{V}_{\Delta\Delta}^{L_\Delta S_\Delta L'_\Delta S'_\Delta}(p_\Delta,q')g_\Delta(q')F_{\Delta N}^{L'_\Delta S'_\Delta L_N S_N}(q',p_N)\ , \tag{A21}$$

with

$$F_{\Delta N}^{L_\Delta S_\Delta L_N S_N}(p_\Delta,p_N)=p_\Delta T_{\Delta N}^{L_\Delta S_\Delta L_N S_N}(p_\Delta,p_N)\ . \tag{A22}$$

By construction, $F_{\Delta N}^{L_\Delta S_\Delta L_N S_N}(p_\Delta,p_N)$ vanishes at the origin and for $p_\Delta=\infty$. This function $F_{\Delta N}^{L_\Delta S_\Delta L_N S_N}(p_\Delta,p_N)$ may be expanded in the spline functions $S_i(q_i)$ $(i=0,\ldots,2I+1)$, where I gives the number of intervals we divide the domain [50] of p_Δ:

$$F_{\Delta N}^{L_\Delta S_\Delta L_N S_N}(p_\Delta,p_N)=\sum_{i=0}^{2I+1} c_i^{L_\Delta S_\Delta L_N S_N}S_i(p_\Delta)\ . \tag{A23}$$

Let us denote by $\bar{q}_0,\ldots,\bar{q}_I$ the breakpoints that define such intervals. We recall from Refs. [50] and [51] that the S_{2i} $(i=0,\ldots,I)$ splines are even around the $\bar{q}_i$ breakpoint and the S_{2i+1} $(i=0,\ldots,I)$ splines are odd around the same breakpoint. Moreover, both S_{2i} and S_{2i+1} are piecewise cubic polynomials vanishing outside the interval $[\bar{q}_{i-1},\bar{q}_{i+1}]$, and they satisfy the normalization conditions

$$S_{2i}(\bar{q}_i)=1,\quad S_{2i+1}(\bar{q}_i)=0,\quad i=0,\ldots,I\ . \tag{A24}$$

Since $F_{\Delta N}^{L_\Delta S_\Delta L_N S_N}(p_\Delta,p_N)$ vanishes at both $p_\Delta=0$ and ∞ and because of the normalization conditions (A24), the coefficients $c_0^{L_\Delta S_\Delta L_N S_N}$ and $c_{2I}^{L_\Delta S_\Delta L_N S_N}$ must vanish, and the expansion (A23) is reduced to $2I$ terms only, where the splines S_0 and S_{2I} are taken out. If one relabels the S_{2I+1} spline as the S_{2I} one, (A23) becomes

$$F_{\Delta N}^{L_\Delta S_\Delta L_N S_N}(p_\Delta,p_N)=\sum_{i=1}^{2I} c_i^{L_\Delta S_\Delta L_N S_N}S_i(p_\Delta)\ , \tag{A25}$$

which automatically fulfills the correct boundary conditions and which satisfies

$$\sum_{i=1}^{2I} c_i^{L_\Delta S_\Delta L_N S_N}S_i(p_\Delta)=p_\Delta \tilde{V}_{\Delta N}^{L_\Delta S_\Delta L_N S_N}(p_\Delta,p_N)+\sum_{L'_\Delta S'_\Delta}\sum_{i=1}^{2I} c_i^{L'_\Delta S'_\Delta L_N S_N}\int_0^\infty q'\,dq'\,p_\Delta \tilde{V}_{\Delta\Delta}^{L_\Delta S_\Delta L'_\Delta S'_\Delta}(p_\Delta,q')g_\Delta(q')S_i(q')\ . \tag{A26}$$

Discretizing the q dependence and q' integral by defining a mesh $q_1,\ldots,q_{N_q}$ of N_q points with weights $\omega_1,\ldots,\omega_{N_q}$, we end up with

$$\sum_{i=1}^{2I} c_i^{L_\Delta S_\Delta L_N S_N}S_i(p_\Delta)=p_\Delta \tilde{V}_{\Delta N}^{L_\Delta S_\Delta L_N S_N}(p_\Delta,p_N)+\sum_{L'_\Delta S'_\Delta}\sum_{j=1}^{N_q} q_j\omega_j p_\Delta \tilde{V}_{\Delta\Delta}^{L_\Delta S_\Delta L'_\Delta S'_\Delta}(p_\Delta,q_j)g_\Delta(q_j)\sum_{i=1}^{2I} c_i^{L'_\Delta S'_\Delta L_N S_N}S_i(q_j)\ . \tag{A27}$$

We must introduce also a $\{p_k\}$ mesh of inversion to discretize the p_Δ variable. Let N_p be the number of points of this mesh. If we define the matrix elements

$$M_{ki}=S_i(p_k)\ , \tag{A28}$$

$$I_{ki}^{L_\Delta S_\Delta L'_\Delta S'_\Delta}=p_k\sum_{j=1}^{N_q} q_j\omega_j \tilde{V}_{\Delta\Delta}^{L_\Delta S_\Delta L'_\Delta S'_\Delta}(p_k,q_j)g_\Delta(q_j)S_i(q_j)\ , \tag{A29}$$

Eq. (A27) will read

$$\sum_{i=1}^{2I}\sum_{L'_\Delta S'_\Delta}(M_{ki}\delta_{L_\Delta S_\Delta L'_\Delta S'_\Delta}-I_{ki}^{L_\Delta S_\Delta L'_\Delta S'_\Delta})c_i^{L'_\Delta S'_\Delta L_N S_N}=p_k \tilde{V}_{\Delta N}^{L_\Delta S_\Delta L_N S_N}(p_k,q_N),\quad k=1,\ldots,N_p\ . \tag{A30}$$

If N_Δ is the number of Δ channels and N_N the number of nucleon channels, coupled, we have $N_\Delta\times N_N\times 2I$ unknowns. To have the same number of equations, we need to set $N_p=2I$. We did it by defining the mesh of inversion $\{p_k\}$ through the "orthogonal collocation" method: Two Gaussian points are chosen in each of the subintervals we divided in the p range. As for the $\{q_j\}$ mesh of integration, we made the optimal choice from the numerical point of view [51]. We took it to be identical to the $\{p_k\}$ mesh of inversion. We stress that no cutoff parameter was used neither for the inversion matrix mesh $\{p_k\}$ nor for the integration one $\{q_k\}$. To avoid such a truncation, we worked on the [0,1] interval always, to which we mapped the $[0,\infty[$ interval by means of the following change of variables:

$$x=\frac{p_\Delta}{p_\Delta+B},\quad p_\Delta\in[0,\infty[\ , \tag{A31}$$

where B is a constant.

APPENDIX B: DERIVATION OF THE DIFFERENTIAL CROSS SECTIONS (2.16) FOR $pp\to(\pi^+p)$ AND $\pi^+d\to(\pi^+p)n$

In what follows and as stated in Sec. II A $\phi_0(\mathbf{p}',\mathbf{q}')$ denotes the three-body πNN final state in terms of a set of Jacobi coordinates. We have chosen this set to be

$$\mathbf{p}'=\frac{\omega_\pi(q_\pi)/c^2\mathbf{k}_N-m_N\mathbf{q}_\pi}{m_N+\omega_\pi(q_\pi)/c^2}\ , \tag{B1a}$$

$$\mathbf{q}'=\mathbf{k}_N+\mathbf{q}_\pi=-\mathbf{p}_f\ , \tag{B1b}$$

with

$$\omega_\pi(q_\pi)=(m_\pi^2c^4+q_\pi^2c^2)^{1/2}\ , \tag{B1c}$$

where $\mathbf{k}_N$ and $\mathbf{p}_f$ stand for the momentum of the interacting and spectator nucleons, respectively.

Equations (B1) allow us to split the πN system energy into its relative and c.m. kinetic energy, which is only approximately relativistically correct. The differential cross section for the breakup $NN\to NN\pi$ reaction reads, according to (2.15a),

$$d^6\sigma_{pp\to(\pi^+p)n}=(2\pi)^4\frac{\mu_N(p_N)}{\hbar^2}\frac{1}{p_N}\delta(E_0-2e_N(p_N))d^3p'\,d^3q'|\langle\phi_0(\mathbf{p}',\mathbf{q}')|U_{0N}(2e_N(p_N)+i0)|\phi_N(\mathbf{p}_N)\rangle|^2\ . \tag{B2}$$

For the calculation of the matrix element

$$\langle\phi_0(\mathbf{p}',\mathbf{q}')|U_{0N}(2e_N(p_N)+i0)|\phi_N(\mathbf{p}_N)\rangle\ ,$$

we only take into account the process in which the final (π^+p) state is produced by the decay of a double-charged Δ^{++} state. The contribution from the background process via the decay of a single-charged Δ^+ state is neglected.

Two vectorial integrations must be performed in Eq. (B2). The integration over p'^2dp' is trivial because of the delta function. The range of integration of q'^2dq' is in general determined by the experimental arrangement that contains a definite delta mass range. We must at this point clarify that we carry out the integration over the experimentally measured kinematic domain of q' according to Ref. [2]. By substituting Eq. (2.11) into (B2), we get, after averaging over initial and final spins and taking into account the identity of nucleons in the final state,

$$\begin{aligned}\frac{d\sigma_{pp\to(\pi^+p)n}}{d\Omega_{q'}}&=(2\pi)^4\frac{\mu_N(p_N)}{\hbar^2}\frac{1}{p_N}\frac{2}{4}\frac{3}{4\pi}\\&\times\int d\Omega_{p'}\boldsymbol{\sigma}_{N\Delta}(2)\cdot\mathbf{p}'\boldsymbol{\sigma}_{N\Delta}(2)\cdot\mathbf{p}'\\&\times\tfrac{3}{4}\int_0^\infty p'^2dp'\langle f|\mathbf{p}'\rangle\langle\mathbf{p}'|f\rangle\int q'^2dq'\frac{\delta(E_0-2e_N(p_N))|\langle\mathbf{q}'|T_{\Delta N}(2e_N(p_N)+i0)|\phi_N(\mathbf{p}_N)\rangle|^2}{|2e_N(p_N)+i0-e_N(q')-\Sigma_\Delta(2e_N(p_N)-e_N(q'),q')|^2}\ ,\end{aligned} \tag{B3}$$

where the factors $3/4\pi$ and $\frac{3}{4}$ arise from a normalization factor of the $\pi N\Delta$ vertex, $\langle p'|f\rangle$, and the isospin matrix element, respectively. The proper antisymmetrization of the two nucleons in the final state yields an extra factor of 2 in Eq. (B3).

To proceed further one needs to perform the p'^2dp' integration in Eq. (B3). The self-energy correction $\Sigma_\Delta(\varepsilon_\Delta,k_\Delta)$ of the Δ isobar is defined in its structure by Eq. (2.1), i.e.,

$$\Sigma_\Delta(\varepsilon,q')=M_\Delta(\varepsilon,q')+\frac{q'^2}{2m_\Delta}-\frac{i}{2}\Gamma_\Delta(\varepsilon,q')\ . \tag{B4}$$

It is calculated from a model where the P_{33} interaction is described by a separable πN interaction, through the underlying form factor $\langle f|p\rangle$; we have [3]

$$M_\Delta(\epsilon,q')-\frac{i}{2}\Gamma_\Delta(\varepsilon,q')=m_\Delta c^2+\int_0^\infty p'^2dp'\frac{\langle f|p'\rangle\langle p'|f\rangle}{\varepsilon-\omega_\pi(p')-e_N(p')-\hbar^2q'^2/2[m_N+\omega_\pi(p')/c^2]+i0}\ , \tag{B5}$$

from which we are able to conclude that the width $\Gamma_\Delta(\varepsilon,q')$ is what remains from the integral in Eq. (B5), once the prin-

cipal value is removed. That amounts to have

$$\Gamma_\Delta(\varepsilon,q')=2\pi\int_0^\infty p'^2dp'\langle f|p'\rangle\delta\left[\varepsilon-\omega_\pi(p')-e_N(p')-\frac{\hbar^2q'^2}{2[m_N+\omega_\pi(p')/c^2]}\right]\langle p'|f\rangle\ . \tag{B6}$$

Since

$$\delta(E_0-2e_N(p_N))=\delta\left[2e_N(p_N)-e_N(p')-\omega_\pi(p')-e_N(q')-\frac{\hbar^2q'^2}{2[m_N+\omega_\pi(p')/c^2]}\right]\ , \tag{B7}$$

where the energy available for Δ excitation is $\varepsilon=2e_N(p_N)-e_N(q')$ ($e_N(p')+\omega_\pi(p')$ describes the relative motion of the πN system and $\hbar^2q'^2/2[m_N+\omega_\pi(p')/c^2]$ its c.m. motion), we have

$$\int_0^\infty p'^2dp'\langle f|p'\rangle\delta(E_0-2e_N(p_N))\langle p'|f\rangle=\frac{\Gamma_\Delta}{2\pi}(\varepsilon,q')\ . \tag{B8}$$

On the other hand, because of (B4) and as already mentioned in Sec. II A,

$$-\frac{\Gamma_\Delta}{2}(\varepsilon,q')\frac{1}{|\varepsilon-\Sigma_\Delta(\varepsilon,q')|^2}=\mathrm{Im}\frac{1}{\varepsilon-\Sigma_\Delta(\varepsilon,q')}=\mathrm{Im}G_\Delta(\varepsilon,q')\ . \tag{B9}$$

From Eqs. (B8) and (B9), it follows that (B3) gives

$$\frac{d^3\sigma_{pp\to(\pi^+p)n}}{d^3/dq'^3}=(2\pi)^4\frac{\mu_N(p_N)}{\hbar^2}\frac{1}{p_N}\frac{2}{4}\frac{3}{4\pi}\frac{3}{4}(-1)\frac{1}{\pi}\mathrm{Im}G_\Delta(\varepsilon,q')|\langle\mathbf{q}'|T_{\Delta N}(2e_N(p_N)+i0)|\phi_N(\mathbf{p}_N)\rangle|^2\ , \tag{B10}$$

which is the result given in Eq. (2.16).

[1] M. T. Peña, H. Henning, and P. U. Sauer, Phys. Rev. C **42**, 850 (1990).

[2] A. B. Wicklund *et al.*, Phys. Rev. D **35**, 1670 (1987).

[3] H. Pöpping, P. U. Sauer, and Zhang Xi-Zhen, Nucl. Phys. **A474**, 557 (1987).

[4] T.-S. H. Lee, Phys. Rev. C **29**, 195 (1984); T.-S. H. Lee and A. Matsuyama, *ibid.* **32**, 516 (1985); **32**, 1986 (1985); **36**, 1459 (1987).

[5] U. Oelfke, Ph.D. dissertation, University of Hannover, 1990.

[6] U. Oelfke and P. U. Sauer (unpublished).

[7] E. O. Alt, P. Grassberger, and W. Sandhas, Nucl. Phys. **B2**, 167 (1967).

[8] W. M. Kloet, R. R. Silbar, R. Aaron, and R. D. Amado, Phys. Rev. Lett. **39**, 1643 (1977); W. M. Kloet and R. R. Silbar, *ibid.* **45**, 970 (1980); Nucl. Phys. **A338**, 281 (1980); **A364**, 346 (1981); J. Dubach, W. M. Kloet, and R. R. Silbar, J. Phys. G **8**, 475 (1982); Phys. Rev. C **33**, 373 (1986); Nucl. Phys. **A445**, 537 (1987).

[9] T. Mizutani and D. S. Koltun, Ann. Phys. (N.Y.) **109**, 1 (1977); Y. Avishai and T. Mizutani, Nucl. Phys. **A326**, 352 (1979); **A338**, 377 (1980); **A352**, 399 (1981); C. Fayard, G. H. Lamot, and T. Mizutani, Phys. Rev. Lett. **45**, 524 (1980); N. Giraud, G. H. Lamot, and C. Fayard, *ibid.* **40**, 438 (1978); Phys. Rev. C **21**, 1959 (1980); N. Giraud, Y. Avishai, C. Fayard, and G. H. Lamot, Phys. Lett. **77B**, 141 (1978); Phys. Rev. C **19**, 465 (1979); T. Mizutani, C. Fayard, G. H. Lamot, and S. R. Nahabetian, *ibid.* **24**, 2633 (1981); Phys. Lett. **107B**, 177 (1981); T. Mizutani, B. Saghai, C. Fayard, and G. H. Lamot, Phys. Rev. C **35**, 677 (1987); **40**, 2763 (1989).

[10] A. W. Thomas and I. R. Afnan, Phys. Lett. **45B**, 437 (1973); Phys. Rev. C **10**, 109 (1974); B. Blankleider and I. R. Afnan, *ibid.* **22**, 1638 (1980); **24**, 1572 (1981); **31**, 1380 (1985); **32**, 2006 (1985); Phys. Lett. **93B**, 367 (1980).

[11] A. W. Thomas, Nucl. Phys. **A258**, 417 (1976); A. S. Rinat and A. W. Thomas, *ibid.* **A282**, 365 (1977); Phys. Rev. C **20**, 216 (1979); A. S. Rinat, E. Hammel, Y. Starkand, and A. W. Thomas, Nucl. Phys. **A329**, 285 (1979); A. S. Rinat, E. Starkand, and E. Hammel, Nucl. Phys. **A364**, 486 (1981); A. S. Rinat, *ibid.* **A287**, 399 (1977); **A377**, 341 (1982); A. S. Rinat and E. Starkand, *ibid.* **A397**, 381 (1983); A. S. Rinat and Y. Alexander, *ibid.* **A404**, 467 (1983); B. J. Jennings and S. Rinat, *ibid.* **A485**, 421 (1988).

[12] M. Araki, Y. Koike, and T. Ueda, Prog. Theor. Phys. **63**, 335 (1980); **63**, 2133 (1980); M. Araki and T. Ueda, Nucl. Phys. **A379**, 449 (1982); **A389**, 605 (1983); T. Ueda, Prog. Theor. Phys. **76**, 959 (1986); **76**, 729 (1986); Phys. Lett. **74B**, 123 (1978); **119B**, 281 (1982); **141B**, 157 (1984); Phys. Lett. B **175**, 19 (1986); Nucl. Phys. **A463**, 69c (1987).

[13] J. M. Rivera and H. Garcilazo, Nucl. Phys. **A285**, 505 (1977); H. Garcilazo, Phys. Rev. C **35**, 1804 (1987); Phys. Rev. Lett. **45**, 780 (1980); **48**, 577 (1982); **53**, 652 (1984); **61**, 1457 (1988); **65**, 293 (1990); A. W. Thomas, Nucl. Phys. **A258**, 417 (1976).

[14] N. Tanabe and K. Otha, Phys. Rev. C **36**, 2495 (1987); Phys. Rev. Lett. **56**, 2785 (1986); Nucl. Phys. **A484**, 493 (1988).

[15] T. Mizutani and H. Garcilazo, *πNN Systems* (World Scientific, Singapore, 1990).

[16] H. Garcilazo, T. Mizutani, M. T. Peña, and P. U. Sauer, Phys. Rev. C **42**, 2315 (1990).

[17] M. Lacombe, B. Loiseau, J. M. Richard, R. Vinh Mau, J. Côté, P. Pirès, and R. de Tourreil, Phys. Rev. C **21**, 861

(1980).
[18] A. Bulla, Ph.D. dissertation, University of Hannover, 1990.
[19] T.-S. H. Lee, Phys. Rev. Lett. **50**, 1571 (1983).
[20] R. Machleidt, K. Holinde, and Ch. Elster, Phys. Rep. **149**, 1 (1987).
[21] S. C. B. Andrade, E. Ferreira, and H. G. Dosch, Phys. Rev. C **34**, 226 (1986); E. Ferreira, S. C. B. Andrade, and H. G. Dosch, *ibid.* **36**, 1916 (1987).
[22] C. Alexandrou and B. Blankleider, Phys. Rev. C **42**, 517 (1990).
[23] H. Garcilazo, Phys. Rev. C **42**, 2334 (1990).
[24] Ch. Hajduk, P. U. Sauer, and W. Strueve, Nucl. Phys. **A405**, 581 (1983).
[25] W. Strueve, Ch. Hajduk, P. U. Sauer, and W. Theis, Nucl. Phys. **A465**, 651 (1987).
[26] H. Pöpping, P. U. Sauer, and Zhang Xi-Xhen (unpublished).
[27] R. A. Arndt, L. Roper, R. Bryan, R. Clark, B. Verwest, and P. Signell, Phys. Rev. D **28**, 97 (1983).
[28] D. V. Bugg, A. Hasan, and R. L. Shypit, Nucl. Phys. **A477**, 576 (1988).
[29] R. Gabathuler *et al.*, Nucl. Phys. **A350**, 253 (1980).
[30] C. Ottermann, E. T. Boschitz, W. Gyles, W. List, and R. Tacik, Phys. Rev. C **32**, 928 (1985).
[31] G. R. Smith, E. L. Mathie, E. T. Boschitz, and C. Ottermann, Phys. Rev. C **29**, 2206 (1984).
[32] E. Ungricht, W. S. Freeman, D. F. Geesaman, R. J. Holt, J. R. Specht, and B. Zeidman, Phys. Rev. C **31**, 934 (1985).
[33] Y. M. Shin, K. Itoh, N. R. Stevenson, D. R. Gill, D. F. Ottewell, G. D. Wait, T. E. Drake, D. F. Frakers, R. B. Schubank, and G. J. Lolos, Phys. Rev. Lett. **55**, 2672 (1985).
[34] A. B. Laptev and I. I. Strakovsky, Leningrad Nuclear Physics Institute report, 1985.
[35] G. R. Smith *et al.*, Phys. Rev. C **30**, 980 (1984).
[36] J. P. Auger, C. Lazard, and R. J. Lombard, Phys. Rev. D **39**, 763 (1989).
[37] C. Fayard, G. H. Lamot, T. Mizutani, and B. Saghai (in preparation); and as quoted in Ref. [15], pp. 201–203.
[38] H. G. Dosch and E. Ferreira, Phys. Rev. C **38**, 2322 (1988).
[39] R. Kose, W. Paul, and K. Stockhorst, Z. Phys. **202**, 364 (1967).
[40] D. I. Sober, D. G. Cassel, A. J. Sadoff, K. W. Chen, and P. A. Crean, Phys. Rev. Lett. **22**, 430 (1969).
[41] J. Arends, H. J. Gassen, A. Hegerath, B. Mecking, G. Noldeke, P. Prenzel, T. Reichelt, A. Voswinkel, and W. W. Sapp, Nucl. Phys. **A412**, 509 (1984).
[42] P. Dougan, T. Kikivas, K. Lugnér, V. Ramsay, and W. Stifler, Z. Phys. **276**, 55 (1976).
[43] V. G. Gorbenko, Yu. V. Zhebrovskij, L. Ya. Kolesnikov, A. L. Rubashkin, and P. V. Sorokin, Nucl. Phys. **A381**, 330 (1982).
[44] P. Wilhelm, W. Leidemann, and H. Arenhövel, Few-Body Syst. **3**, 111 (1988).
[45] G. V. Holtey, G. Knop, H. Stein, J. Stümpfig, and H. Wahlen, Z. Phys. **259**, 51 (1973).
[46] B. Bouquet, J. Buon, B. Grelaud, H. Guyen'ngoc, P. Petroff, R. Riskalla, and R. Tchapoutian, Nucl. Phys. **B79**, 45 (1974).
[47] A. Matsuyama, Phys. Lett. **152B**, 42 (1985).
[48] A. Matsuyama and T.-S. H. Lee, Phys. Rev. C **34**, 1900 (1986).
[49] A. J. Huizing and B. L. B. Bakker, J. Comput. Phys. **90**, 200 (1980).
[50] G. R. Payne, in *Models and Methods in Few Body Physics*, edited by L. S. Ferreira, A. C. Fonseca, and L. Streit (Springer, New York, 1987), Vol. 275.
[51] G. D. Bosveld and N. W. Schellingerhout, Master's thesis, University of Groningen, 1979.